CEBAF Program Advisory Committee Six (PAC6) Proposal Cover Sheet

This proposal must be received by close of business on April 5, 1993 at:

CEBAF

User Liaison Office

12000 Jefferson Avenue

Newport News, VA 23606

Proposal Title

Photoproduction of Vector Mesons
at High t

Contact Person

Name: MARCHAND Claude

Institution: CE SACLAY

Address: DSM/DAPNIA/SPhN

Address: Batiment 703, Orme des Merisiers

City, State ZIP/Country: 91191 GIF/YVETTE CEDEX, FRANCE

Phone: (33) 1 69 08 86 59 **FAX:** (33) 1 69 08 73 54

E-Mail → BITnet: MARCHAND at FRSAC11 **Internet:**

If this proposal is based on a previously submitted proposal or letter-of-intent, give the number, title and date:

CEBAF Use Only

Receipt Date: 4/5/93 Log Number Assigned: PR 93-031

By: gp

April 02, 1993

Photoproduction of Vector Mesons at High t

G. Audit, A. Boudard, P. Couvert, G. Fournier, F. Kunne, J.M. Laget[*‡], C. Marchand[†], R. Mendez-Galain, B. Saghai

Service de Physique Nucléaire, Centre d'Etude de Saclay

F91191, Gif-sur-Yvette CEDEX, France

M. Anghinolfi[*], G. Ricco, P. Corvisiero, L. Mazzaschi, V.I. Mokeev, M. Ripani, M. Sanzone, M. Taiuti and A. Zucchiatti

INFN-Sezione di Genova e Dipartimento di Fisica dell'Università

Genova, Italy

R. Frascaria[a], M.Morlet[a], J. Van de Wiele[a]

Institut de Physique Nucléaire

F91406, Orsay CEDEX, France

B.L Berman, W.J. Briscoe, P.L. Cole, J.P Connelly, K.S. Dhuga, W.R. Dodge and S.L. Rugari

Center for Nuclear Studies, The George Washington University

Washington, DC20052, USA

G.S. Blanpied, C. Djalali, M. Guidal, B. Preedom, A. Tam, C.S. Whisnant

Physics Department, University of South Carolina

Columbia, SC29208, USA

G. Adams, J. Napolitano, P. Stoler and B. Wojtsekowski

Physics Department, Rensselaer Polytechnic Institut

Troy, NY12180, USA

[*] Spokespersons

[†] Contact-person

[‡] Will present the proposal

[a] To be confirmed

The main goal of this experiment is to study the photoproduction of ϕ mesons at large t on the nucleon and few-body nuclei. This reaction is expected to proceed via the exchange of two gluons, which provides us with a unique way to study hidden-color components (or more generally correlations between quarks) in hadronic matter. The signature of the ϕ will be its decay into two kaons.

At the same time two pions will also be registered and the study of the production of ρ and ω mesons, as well as $\pi\Delta$ pairs, will enlarge the scope of our research proposal by opening access to other quark rearrangement hard mechanisms. The $K^+\Lambda$ channel will also be clearly identified.

This experiment will make use of a liquid cryogenic target designed in Saclay. It will be run at the highest energy available at CEBAF, and will make use of the CLAS and its photon tagger, with the lower limit of the photon energy set at approximately 3 GeV.

The combined use of an intense high energy monochromatic photon beam and CLAS will allow us to overdetermine the kinematics, by recording events with large multiplicity. This will make it possible to disentangle the relevant channels from the others.

This experiment can be started at the nominal energy $4GeV$ of CEBAF : the total c.m. energy $\sqrt{s}$ and momentum transfer t are already high enough to see the onset of hard processes. In addition, particle identification is simpler than at higher energy. However, it will take full advantage of any significant increase of the CEBAF energy : the study of the variation of the cross section with energy is a way to disentangle different hard mechanisms and to enter more deeply into the relevant domain.

1 The physics case

1.1 Photoproduction of Phi mesons and of Kaon pairs

Since the ϕ meson consists primarily of a strange quark pair, its electro- and photoproduction appear to be an original and straightforward way to make a link between the description of hadronic matter in terms of hadrons and its description in terms of quarks and gluons [1]. On the one hand, its basic constituents are different from the main constituents of nuclear matter : strangeness is a good tag to follow quark rearrangement mechanisms, and to understand how color neutralizes. On the other hand, a possible intrinsic strange component in nuclear matter is still an open question. These two issues are closely related to the short-range properties of nuclear matter.

The threshold for ϕ photoproduction (1.54 GeV) is well below the highest energy available (or expected) at CEBAF. The energy and the momentum transfer can therefore be chosen high enough to look for the onset of hard mechanisms; and real photons make it possible to transfer to the target the highest energy available at CEBAF.

At low momentum transfer (emission at forward angles), this is a purely diffractive process which depends only on the sizes of the ϕ and the target : it can be described by the

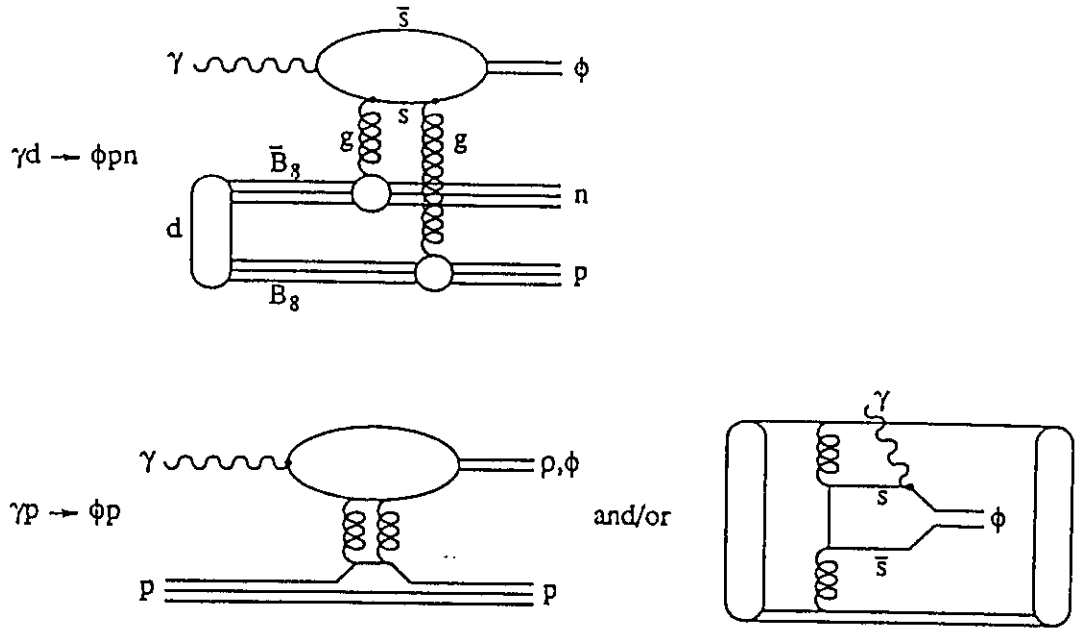

Figure 1: *Possible two gluon exchange mechanisms which could be responsible of Φ photo and electroproduction on deuterium (top) and free nucleon (bottom). The notations B_8 and $\overline{B_8}$ stand for colored quark clusters. The contribution of a possible intrinsic strange component is depicted on the right.*

exchange of the Pomeron Regge trajectory. At large momentum transfer (above 1 GeV/c), hard processes are expected to take over : the exchange of a "perturbative Pomeron" (two gluons, as depicted in Fig 1), which has already led to a good accounting of ρ electroproduction integrated cross-section at large photon four-momentum (Q^2), appears to be a good candidate [3]. Contrary to ρ meson production, which also involves the interchange of valence quarks, ϕ meson production singles out two gluon exchange mechanisms : they are the simplest possible, provided that ϕ is a pure $s\bar{s}$ state and that the strangeness content of nucleon is small. Increasing the momentum transfer is a way to suppress soft mechanisms and to tune such hard mechanisms. This is a completely open field, which deserves a dedicated study.

The aim of this part of the proposal is twofold : the study of ϕ production on the free nucleon, and the study of its production on few body nuclei.

- Experimental data on ϕ photoproduction on free nucleon are very sparse : they concern only forward angle production or inclusive cross sections. A few angular distributions have been measured (up to $t \sim -1(GeV/c)^2$). This is the first reason to undertake a systematic study, in order to unravel soft and hard processes.The second reason is that it offers us a unique way to study the hard part of the Pomeron (in terms of two gluon exchange) which is also advocated in the analysis of both nucleon-nucleon scattering at asymptotic energies and the nucleon structure function at small

x (see Ref. [3] for a review).

We propose to determine the cross section of the $p(\gamma,\phi)p$ reaction above $-t = 1(GeV/c)^2$, up to $-t \simeq 5(GeV/c)^2$, at the highest energy available at CEBAF.

- If two gluon exchange is the correct mechanism to describe ϕ production, it offers us a way to unravel the short-range hidden-color component of the wave function of the few-body systems. Each gluon can thus couple with a single quark which belongs to a colored cluster (Fig 1). Since such a coupling changes the color, the exchange of the two gluons can induce a transition between a hidden-color component (two colored three-quark clusters in the deuterium, for instance) and a colorless asymptotic state (two baryons, for instance).

  The simplest reaction to study is the $D(\gamma,\phi p)n$ reaction. However one has to suppress the trivial quasi free contribution : it strongly decreases when the momentum of the undetected neutron increases. Above a given neutron momentum the contribution of two-nucleon processes is expected to take over. In order to fully determine the kinematics, the ϕ and the proton must be detected in coincidence.

  Our main goal is to study the $^3He(\gamma,\phi 2p)$ reaction. The quasi-free processes are further suppressed since, contrary to deuterium, the relative wave function of a pp pair at rest in ^3He has no D-wave component : hard components of the wave function (or, equivalently, hard mechanisms) are therefore easier to single out. Moreover, the detection of two protons in coincidence with the ϕ completely determine the kinematics of its photoproduction on a pair of protons.

In both cases, the determination of the density matrix of the emitted ϕ is particularly interesting. Any departure from the s-Channel Helicity Conservation (SCHC), which holds in the pure Vector Meson Dominance Model (VDM) and in the two gluon exchange mechanism, would be the hint for possible other hard processes involving the strange quarks of the sea (intrinsic strange component). The determination of the angular distribution of the two kaons, emitted at the ϕ peak, will be the way to achieve this goal.

In addition, this also allows to determine the relative amount of two kaons emitted in a relative S-state, both in and away from the ϕ peak. Here, interferences between S and P waves are the signature of the breakdown of SCHC. However, the production of two kaons in a relative S-state is interesting in its own right : possible exotic states are predicted to be strongly coupled to this channel.

1.2 Photoproduction of Rho mesons and of Pion pairs

Beside two gluon exchange mechanisms, quark interchange mechanisms may also play a significant role in photoproduction of ρ mesons or pion pairs [2].

Evidences for such hard mechanisms (Fig. 2) already exist in several high energy meson photoproduction reactions. Typical examples are the $\gamma p \to n\pi^+$, $\gamma p \to p\rho$, $\gamma p \to p\omega$

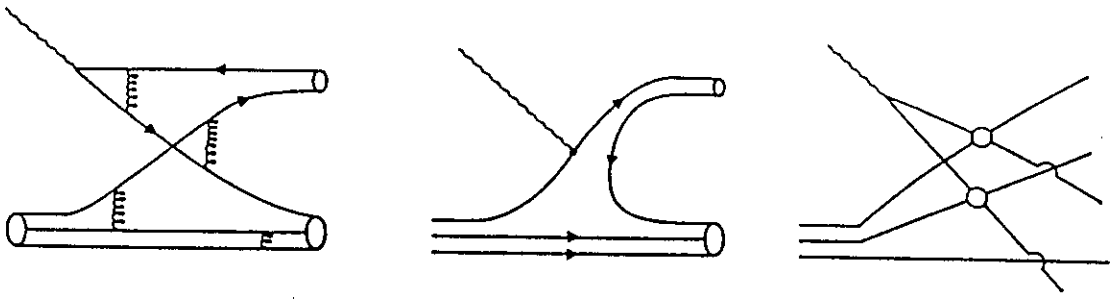

Figure 2: *The diagrams describing hard scatterings between the photon and the nucleon constituents : Vector Meson Dominance hard scattering (left), point like photon coupling (center), Vector Meson multiple Landshoff mechanism (right). In each case the characteristic power law is indicated.*

and $\gamma p \rightarrow \pi^- \Delta^{++}$ reactions which have been studied at SLAC in the energy range $3 < E_\gamma < 8GeV$ and Daresbury in the energy range $3 < E_\gamma < 5GeV$. For large values of P_T, they exhibit a characteristic s^{-8} asymptotic behavior.

A CW beam is necessary to verify this conjecture in a more systematic way. The reactions $\gamma p \rightarrow \Delta^{++}\pi^-$ and $\gamma p \rightarrow \omega p$ were studied with a tagged photon beam of $10^5\gamma/s$ (due to the low duty factor of 5%) at the Daresbury machine. A continuous electron beam allows to increase this figure by two orders of magnitude, up to a few $10^7\gamma/s$, and to perform the experiments on a free nucleon target with higher accuracy and at higher values of P_T.

Due to its large acceptance, the CLAS calorimeter also represents the ideal detector to measure the decay angular distributions of the ρ meson or the Δ. These distributions expressed, for unpolarized photons, in terms of three spin-space density matrix elements could give sufficient information to discriminate among different production mechanisms.

The study of short range quark rearrangement mechanisms in nuclei, requires the selection of kinematics where at least two nucleons are active and where hard scatterings have already been observed in reactions induced on free nucleons. A possible example would be the comparison between the reactions $\gamma D \rightarrow \Delta^{++}\pi^- n$ and $\gamma p \rightarrow \Delta^{++}\pi^-$. The value of the transverse momentum of the emitted Δ^{++} must be large in order to select a hard scattering and the momentum of the neutron must be large enough in order to suppress the quasi-free mechanism (where the neutron is spectator). Other reactions will also be studied at high values of P_T as for instance the $\gamma D \rightarrow \Delta^{++}\Delta^-$ and the $\gamma D \rightarrow (\rho/\omega)pn$ reactions. The study of the reactions $^3He(\gamma, \Delta^{++}\Delta^0)n$ and $^3He(\gamma, (\rho/\omega)pp)n$, which represents an extension toward the high energy region of the proposal on the study of photoreactions in ^3He, are particularly appealing, since all the active particles in the final state are charged and since the higher density of the target makes hard mechanisms more likely.

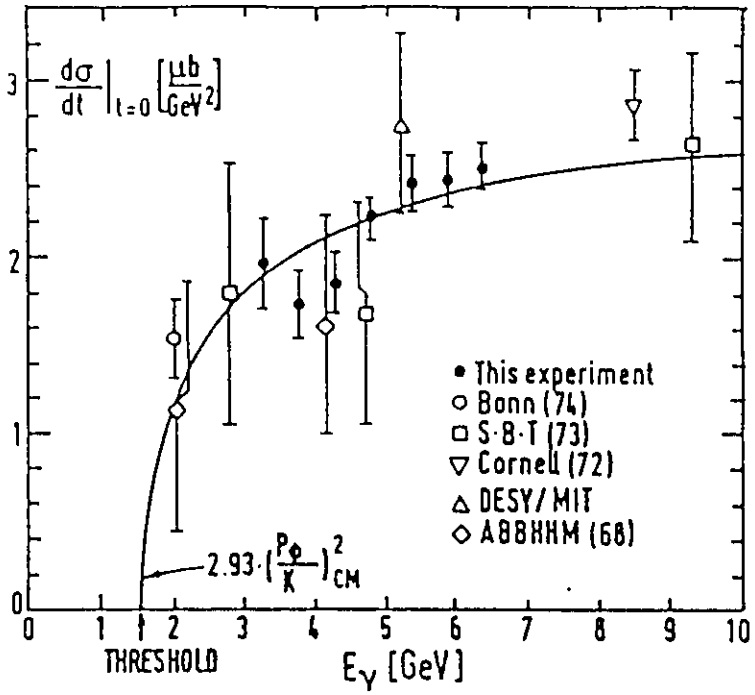

Figure 3: *The forward angle cross section of the $\gamma p \rightarrow \phi p$ reaction is plotted against the photon energy.*

2 Theoretical framework and open questions

2.1 Production of Phi Mesons at Low t.

At low momentum transfer ($-t \leq 0.4$ (GeV/c)^2) , the cross section of the $\gamma p \rightarrow \phi p$ reaction is purely diffractive and takes the form [4,5] :

$$\frac{d\sigma}{dt} = \left(\frac{d\sigma}{dt}\right)_{t=0} exp(Bt) \tag{2.1}$$

The variation with the incoming photon energy of the forward angle ($t = 0$) cross section is shown in Fig. 3. It exhibits a characteristic threshold behavior at low energy and becomes almost constant above $E_\gamma = 6$ GeV. A very good fit is obtained with the following expression :

$$\left(\frac{d\sigma}{dt}\right)_{t=0} = C\left(\frac{p_\phi}{k}\right)^2_{CM} \tag{2.2}$$

with $C = 2.93 \pm 0.08 \mu b/GeV^2$.

When the photon energy is large enough ($E_\gamma \geq 5$ GeV) to avoid trivial threshold behavior, the cross section exhibits a universal momentum dependence (Fig. 4) and a change of slope around $-t = 0.4(GeV/c)^2$: below $-t = 0.4(GeV/c)^2$, the slope parameter take the value $B = 6 \pm 0.5(GeV/c)^{-2}$ and $B \simeq 4(GeV/c)^{-2}$ above. A structure has also been reported [5] around $-t = 0.4(GeV/c)^2$.

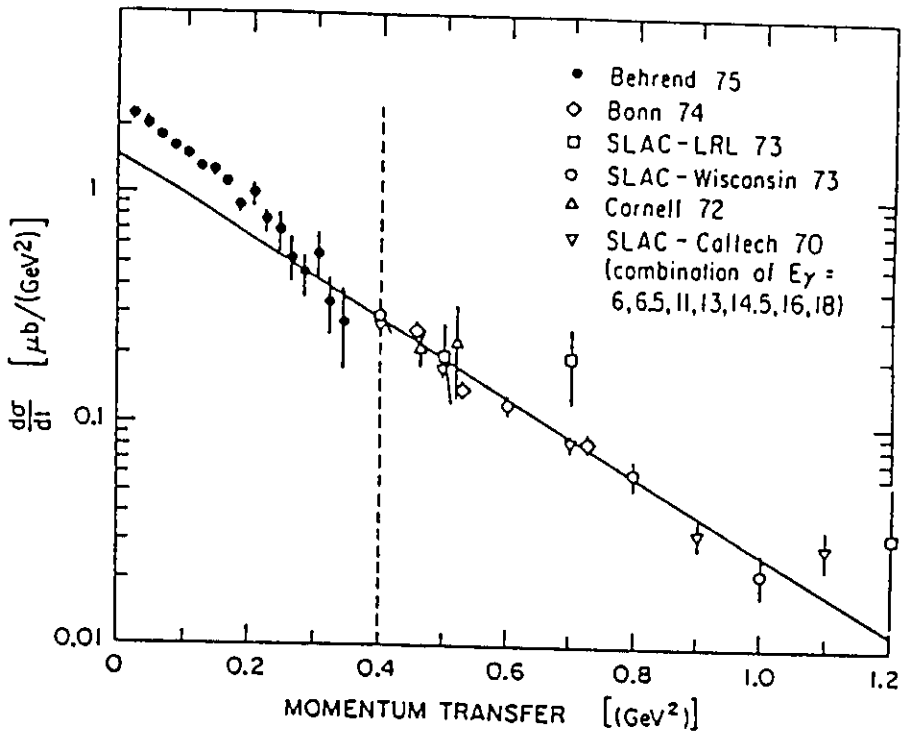

Figure 4: *The cross section of the $\gamma p \rightarrow \phi p$ reaction is plotted against the momentum transfer t.*

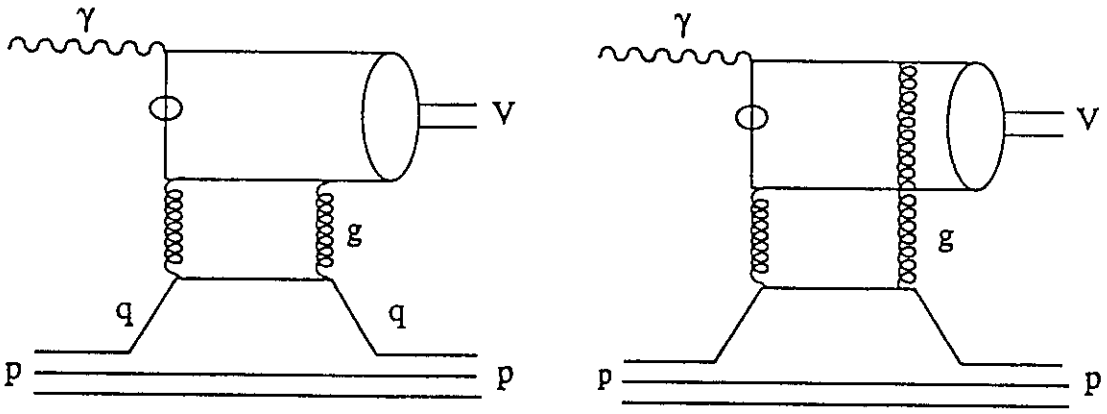

Figure 5: *The two gluon exchange mechanisms which survive at high energy in ϕ photo and electroproduction on free nucleon.*

2.2 Extrapolations at High t.

Above $-t = 1(GeV/c)^2$, no experimental data exist and we have used the two gluon exchange model (Fig. 5) to extrapolate. In the limit $\nu \rightarrow \infty$ the amplitude reduces to the simple form [6,7,8] :

$$A = KF_1(t) \int dl^2 \frac{-4l^2 + t}{(m_\phi^2 + Q^2 - 4l^2)(m_\phi^2 + Q^2 - t)} \left[D(l^2 + \frac{1}{4}t) \right]^2 \qquad (2.3)$$

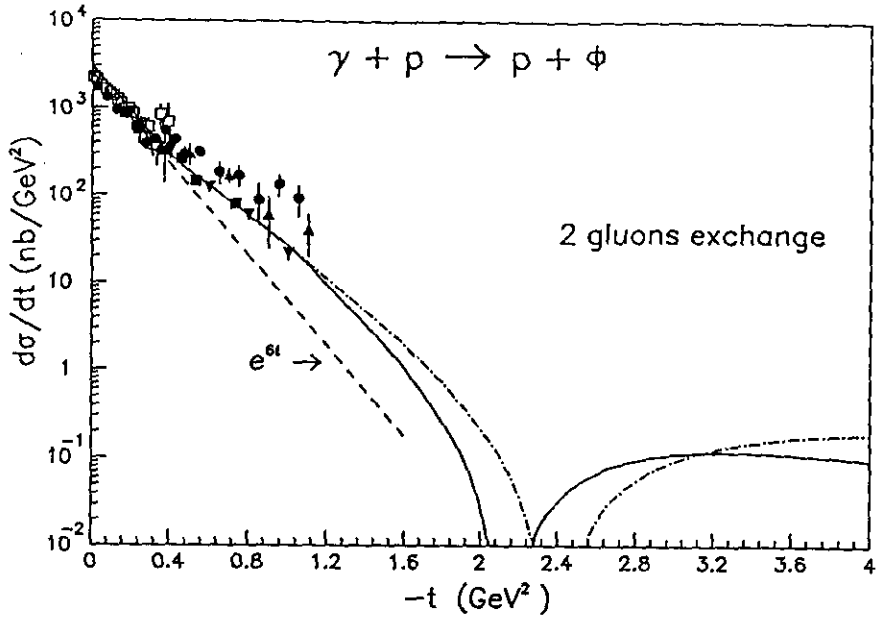

Figure 6: *The cross section of the $\gamma p \to \phi p$ reaction is plotted against t. The dashed line corresponds to the parameterization of the existing experimental data below $-t = 0.4 GeV/c$, in the framework of the VDM model. The dot-dashed line corresponds to the two gluon exchange mechanism as computed in Eq. 2.4. The full line corresponds to the exact amplitude Eq. 2.3.*

It is made of three part. The first is a constant factor K which depends on the various coupling constants and the static properties of the ϕ. The second is the proton form factor $F_1(t)$ which insures that the outgoing proton remains in its ground state. The third is the integral, over the transverse momentum, which describes the exchange of two gluons. The two terms which appear in the denominator correspond to the propagators of the far off-shell quarks marked by a circle in each graph of Fig. 5 : in Eq. 2.3 their amplitudes have been combined in a compact expression. The analysis of the asymptotic high energy behavior of pp scattering, of the small x behavior of the nucleon structure function and the value of the gluon condensate determine the low momentum behavior of the gluon propagator $D(l^2)$ (see [3] for a review). This regularization procedure introduces a momentum scale $\mu_0^2 \approx (1.2 \pm 0.5) GeV^2$ and consequently a gluon correlation length $a \simeq 0.2 fm$: the gluon cannot propagate beyond this distance (this does not mean that all the constituent quarks of the ϕ and proton should lie within this distance, but rather that only one strange quark of the ϕ and one quark from the proton should be close enough). The integral can be done in an approximate way [6] and the momentum dependence of the cross section takes the simple form :

$$\frac{d\sigma}{dt} \propto \left| \frac{2\mu_0^2 + t}{(m_\phi^2 + Q^2 + 2\mu_0^2)(m_\phi^2 + Q^2 - t)} F_1(t) \right|^2 \tag{2.4}$$

where the proton form factor has the following expression :

$$F_1(t) = \frac{4m_p^2 - 2.8t}{(4m_p^2 - t)(1 - t/0.7)^2} \tag{2.5}$$

When integrated against t, these expressions lead to a fair agreement not only with both the magnitude and the Q^2 dependence of the cross section of the $p(e,e')\rho p$ reaction [9] and of the cross section of the $p(\mu,\mu')\rho p$ reaction [10], but also with the density matrix of the final decay $\rho \rightarrow \pi^+\pi^-$. It turns out that this model reproduces also the main trend of the magnitude as well as the t dependence of the cross section of the $\gamma p \rightarrow \phi p$ in the range $0.6 \leq -t \leq 1(GeV/c)^2$: the curves in Fig. 6 have been normalized to the experimental data at $-t = 0.6(GeV/c)^2$.

The t dependence has never been checked and this remains to be done. As it is apparent in Eq. 2.4 the cross section exhibits a node at $t = -2\mu_0^2 \simeq -2.4(GeV/c)^2$ in Fig. 6. It results from the cancellation between the direct two gluon exchange graph (Fig. 5), where the two gluons couple to the same strange quark in the ϕ, and the crossed graph where each gluon couples to a different strange quark in the ϕ. This feature survives when the integral in Eq. 2.3 is performed exactly [14]. Whether this node is an artifact of the approximations (high energy limit,...) which have been made to derive Eq. 2.3, or whether it is a genuine signature of two gluon exchange mechanisms is an open problem. On the other hand, other hard scatterings may also play a role and fill in or shift the corresponding minimum. This certainly deserves a dedicated experimental study.

2.3 Production of Kaon Pairs in the Continuum

Two kaon photoproduction also exhibits interesting features. Figure 7 shows the spectrum [5] of the mass of the two Kaons emitted in the $p(\gamma,K^+K^-)p$ reaction at $E_\gamma = 5$ GeV : the ϕ meson peak clearly appears above the two kaon continuum. The behavior of the spin density matrix elements, which can be determined from the polar and azimuthal angular distributions of the two detected Kaons, is particularly striking : one of them (Y_{10}) exhibits an interference pattern between the S and P waves in the helicity zero channel. Such an interference implies that transverse (helicity one) real photons produce longitudinally polarized (helicity zero) ϕ. This is not allowed in the diffractive Vector Meson Dominance model or in the two gluon exchange model which we just considered. This could be the hint of hard mechanisms, which involve the strangeness content of the nucleon. For instance, the incoming photon can interact directly with a strange quark of the sea (bottom right graph in Fig. 1) and eject a ϕ meson or a correlated Kaon pair in the final state. Such a process is not expected to respect SCHC rule.

The study of the two Kaon continuum is also interesting in itself. On the one hand, the coupling between the two pion and the two kaon channels [11] may induce interesting structures which would correspond to S-wave $K\overline{K}$ molecules. Such molecules are also predicted in quark models [12,13]. On the other hand, the a_0 and f_0 resonances lie very close to the $2K$ threshold and decay into two Kaons.

All these issues are open and have only been partially investigated at low t. The production and decay of such objects at high t is a completely virgin field. Its study will

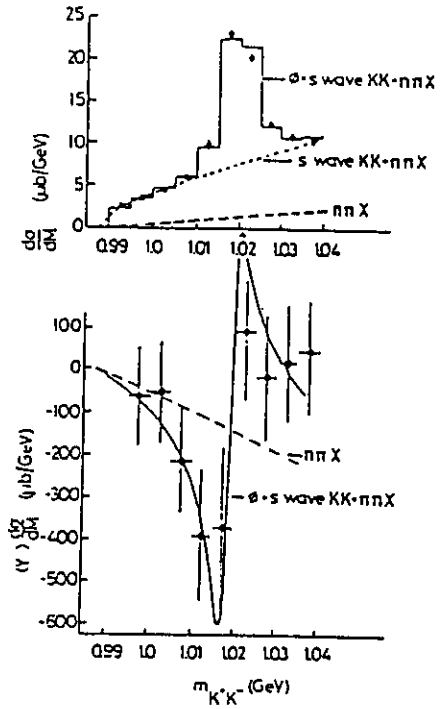

Figure 7: *The mass spectrum of the Kaon pair emitted in the $p(\gamma, K^+K^-)p$ at $E_\gamma = 5$ GeV (top). The Y_{10} spin moment (bottom). See ref. [5] for more details.*

be undertaken at the same time and with the same apparatus as the study of ϕ meson production.

2.4 Production of ρ Meson at High t

It turns out that this two gluon exchange model reproduces [14] not only the ratio between the cross section of the $p(\gamma,\rho)p$ and $p(\gamma,\phi)p$ reactions around $-t = 1(GeV/c)^2$, but also the magnitude of the high t cross section of the $p(\gamma,\rho)p$ reaction. In Fig. 8, the peak at forward angles is due to purely diffractive mechanisms, while the peak at backward angle is due to the exchange of the nucleon Regge trajectory. The latter does not appear in the $p(\gamma,\phi)p$ reaction, since the ϕ couples very weakly to the nucleon. In between, a few points have been measured at high t at SLAC [15]. The fair agreement between the model and the data in these kinematics gives us some confidence in the model, at least to extrapolate and estimate counting rates.

However, quark rearrangement mechanisms (Fig. 2), which are forbidden in ϕ meson production reactions, may also contribute. They should exhibit a s^{-8} or s^{-7} energy dependence. At $E_\gamma = 6GeV$ their contribution may be smaller than, or as small as, the two gluon contribution and only fills in its minimum. At a lower energy their contribution should be more important and could well overwhelm the two gluon contribution.

It should also be noted that these sparse high t data have been obtained with a

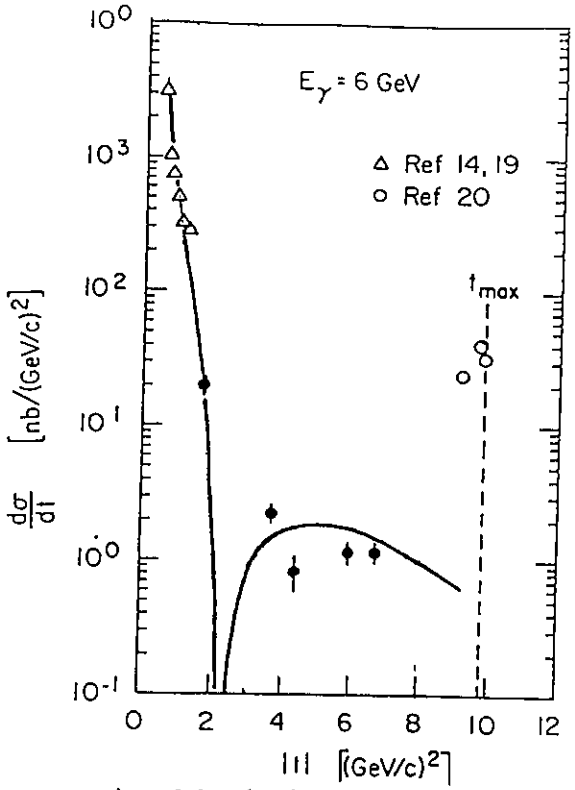

Figure 8: *The cross-section of the $p(\gamma,\rho)p$ reaction at $E_\gamma = 6GeV$. The curve is the prediction of the two gluon exchange model.*

bremssthralhung photon beam by detecting the recoil proton. Preventing to reconstruct the energy distribution of the ρ meson and to disentangle its contribution from the non resonant 2π continuum.

As in the ϕ meson production sector, the determination of the ρ meson decay distributions would be a way to obtain its various helicity components and provide additional informations about the space-momentum region where hard scatterings become dominant. In the past these distributions have been obtained with low statistic and the error bars were too large to allow any definite conclusion : due to its large acceptance, CLAS is the ideal detector to determine them with a good accuracy, even at high momentum transfer.

For all these reasons, a comparison of the behavior of the cross section of the $p(\gamma,\rho)p$ and $p(\gamma,\phi)p$ reactions not only against t but also against s deserves a dedicated study.

2.5 The Nuclear Case.

When the nucleon is embedded in the nuclear medium, two mechanisms govern the photo- and the electroproduction of ϕ mesons. The first is trivial : the quasi-free production mechanism. The second is much more interesting : the exchange of two gluons, each of them being coupled to a different quark (see Fig. 1). It provides us with a way to look for hidden color components, or more generally to the correlation between two quarks in hadronic matter. A coincidence experiment, for instance $D(\gamma,\phi p)n$ or $^3He(\gamma,\phi 2p)n$, must

be performed to disentangle them.

In order to enhance the effects of possible hidden color components, or to enhance the effects of correlations between quarks, the reaction $^3He(\gamma,\phi 2p)n$ should definitely be studied. The reason is that the target pp pair is almost in a pure $^1S_0$ state, contrary to the deuterium which has a sizable D wave component : the high momentum tail of the quasi-free process is reduced accordingly, leaving more room for the two gluon exchange quark rearrangement processes.

When averaged on the Fermi momentum of the center of mass of the target pp pair, the cross section of the quasi-free process in the γ"pp" $\rightarrow pp\phi$ reaction takes the form :

$$\frac{d\sigma}{dtd\vec{P}_R} \propto \left.\frac{d\sigma}{dt}\right|_{\gamma p\rightarrow\phi p} \rho(\mid \vec{P}_R \mid) \tag{2.6}$$

where $\rho(\mid \vec{P}_R \mid)$ is nothing but the nucleon momentum distribution in the active pp pair in ^3He. It decreases very quickly when the undetected nucleon momentum increases : selecting high values of the recoiling nucleon momentum ($P_R > 200 MeV/c$) is the way to suppress the contribution of such a trivial mechanism.

The cross section, corresponding to the exchange of each of the two gluons with a different quark cluster, is expected to exhibit a more flat momentum distribution, since the recoil momentum is shared between the two nucleons. This is schematically depicted in Fig. 9. However it is very difficult to make a quantitative estimate of its magnitude.

A first crude way would be to write the corresponding cross section as :

$$\frac{d\sigma}{dtd\vec{P}_R} \propto \left.\frac{d\sigma}{dt}\right|_{\gamma p\rightarrow\phi p} \left[\varphi_{cc}(\frac{\vec{P}_R}{2})\right]^2 \frac{F_1^4(\frac{t}{4})}{F_1^2(t)} \tag{2.7}$$

where the fourth power of the nucleon form factor comes from the fact that two nucleons have to recombine, each at the momentum transfer $t/4$. It is assumed that the recoil momentum is equally shared between the two colored clusters whose relative wave function is $\varphi_{cc}(\frac{\vec{P}_R}{2})$: this component of the two nucleon wave function is unknown but the aim of this study is to determine it or at least to put some constraint on it.

A more accurate way would be to introduce the relative wave function of two quarks $\varphi_{qq}(l^2)$ in the expression 2.3 :

$$A = K\frac{F_1^2(\frac{t}{4})}{F_1(t)} \int dl^2 \varphi_{qq}(l^2) \frac{-4l^2+t}{(m_\phi^2+Q^2-4l^2)(m_\phi^2+Q^2-t)} \left[D(l^2+\frac{1}{4}t)\right]^2 \tag{2.8}$$

But again this wave function is not known and the purpose of the experiment is to determine it.

It should be however emphasized that the ratio of the values of the form factor F_1 in Eqs. 2.7 and 2.8 acts as an amplifier of the hidden color component : this ratio is the direct manifestation that, at high t, two gluons prefer to couple to two different clusters rather than to a single cluster. Around $-t = 2(GeV/c)^2$ it takes the value :

$$\frac{F_1^4(\frac{t}{4})}{F_1^2(t)} \simeq 3 \; to \; 4 \tag{2.9}$$

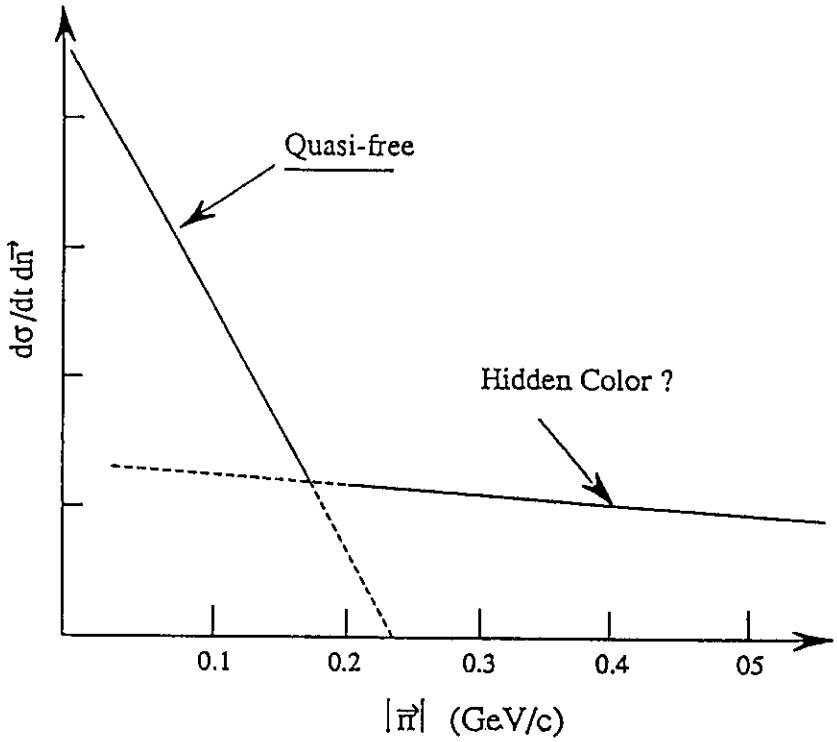

Figure 9: *A schematic representation of the variation with recoil momentum of the cross section of the $D(\gamma, \phi p)n$ reaction.*

When integrated upon $\vec{P_R}$, Eq. 2.6 leads to the free nucleon cross-section, while Eq. 2.7 leads to the free nucleon cross-section multiplied by the probability of hidden component and by the enhancement factor Eq. 2.9. Therefore the ratio between the integral of the tail of the momentum distribution in Fig. 9, which is expected to be dominated above $\mid \vec{P_R} \mid \simeq 150 MeV/c$ by hidden color contributions, and the integral of the quasi free contribution, which vanishes above $150 MeV/c$, represents about three to four times the probability to have a hidden component in the ground-state wave function. Available estimates [16] range around a probability of one per cent. This leads to a ratio of about 3 to 4 percent.

Furthermore, the binning in t should not be as small as in the study of the free nucleon cross-section, since this study will have already determined the domain of validity of the two gluon exchange mechanisms. A binning of $\Delta t \simeq 1(GeV/c)^2$, above $-t = 1(GeV/c)^2$, will increase the counting rate and make it comparable to the counting rate expected on a free nucleon target. A more quantitative estimate is given in section 3.4.

3 Experimental feasibility and counting rates for the reaction $\gamma + p \rightarrow p + \phi$

The main purpose of our study is the photoproduction of ϕ mesons on the nucleon and light nuclei at transfers $-t \geq 1 GeV^2$. We will discuss in this section the experimental

feasibility of such a program on the nucleon with the CLAS detector at both 3.5 and 6 GeV photon energies. After a brief recall of kinematics, we investigate particle identification, phase space, resolutions, background rejection and counting rates.

3.1 Kinematics of the reaction $\gamma + p \rightarrow p + \phi \hookrightarrow K^+K^-$

The reaction we want to study is a typical 2-body reaction, and we chose to detect the ϕ through it's decay channel K^+K^-. The small intrinsic width of the ϕ meson (M_ϕ =1020 MeV, $\Gamma = 4.43$ MeV) allows a clean experimental signature in high background conditions.

Adopting the following convention for four-vector notation:

$$\begin{array}{ccc} & \underline{\gamma} + \underline{p} & \rightarrow \quad \underline{p'} + \underline{\phi} \\ \begin{pmatrix} E_\gamma \\ 0 \\ 0 \\ E_\gamma \end{pmatrix} + \begin{pmatrix} M \\ 0 \\ 0 \\ 0 \end{pmatrix} & \rightarrow & \begin{pmatrix} E' \\ p' \begin{pmatrix} \cos\Phi_p \sin\Theta_p \\ \sin\Phi_p \sin\Theta_p \\ \cos\Theta_p \end{pmatrix} \end{pmatrix} + \begin{pmatrix} E_\phi \\ p_\phi \begin{pmatrix} \cos\Phi_\phi \sin\Theta_\phi \\ \sin\Phi_\phi \sin\Theta_\phi \\ \cos\Theta_\phi \end{pmatrix} \end{pmatrix} \end{array}$$

the center of mass energy squared s and transfer t are :

$$\begin{aligned} s &= (\underline{\gamma} + \underline{p})^2 = M(M + 2E_\gamma) > 0 \\ t &= (\underline{p'} - \underline{p})^2 < 0 \end{aligned}$$

(We use CLAS conventions, that is z along the beam axis).

At photon energies of 3.5 and 6 GeV, the center of mass energy $W = \sqrt{s}$ is equal to 2.7 and 3.5 GeV respectively. At fixed photon energy E_γ, imposing the transfer t fixes the whole 2-body kinematics:

$$\begin{cases} E' = M - \frac{t}{2M} & \rightarrow \quad p' = \sqrt{E'^2 - M^2} \\ E_\phi = E_\gamma + \frac{t}{2M} & \rightarrow \quad p_\phi = \sqrt{E_\phi^2 - M_\phi^2} \end{cases}$$

$$\begin{cases} \cos\Theta_p &= \frac{E_\gamma^2 + p'^2 - p_\phi^2}{2E_\gamma p'} \\ \cos\Theta_\phi &= \frac{E_\gamma^2 + p_\phi^2 - p'^2}{2E_\gamma p_\phi} \end{cases}$$

The transverse momentum $p_\perp$ is defined as:

$$p_\perp = p' \sin\Theta_p = p_\phi \sin\Theta_\phi$$

For a given photon energy E_γ, t and $p_\perp$ are correlated (Figure 10) and have maximum values

$$\begin{cases} t_{max} &= 2M(M_\phi - E_\gamma) \\ p_{\perp\ max} &= \frac{\sqrt{[s-(M_\phi+M)^2][s-(M_\phi-M)^2]}}{2\sqrt{s}} \end{cases}$$

which are $-t_{max} = 4.65$ and 9.35 GeV^2, $p_{\perp\ max} = 0.95$ and 1.44 GeV/c at respectively 3.5 and 6 GeV photon energy.

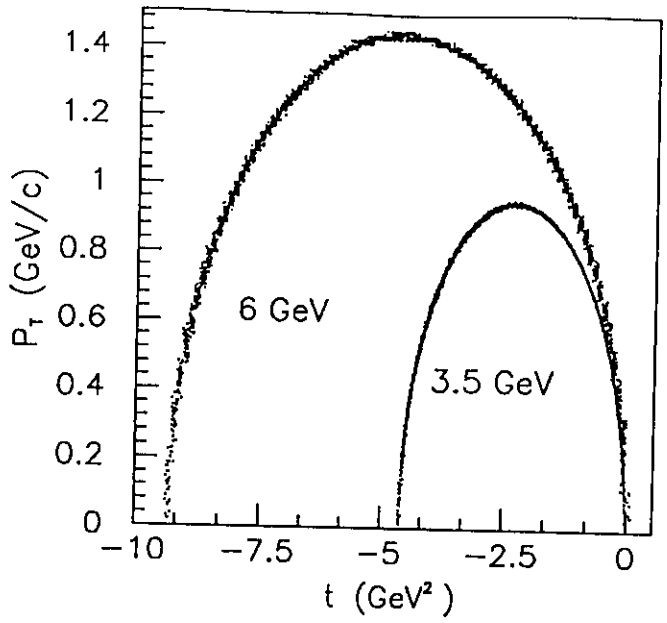

Figure 10: *Transverse momentum $p_\perp$ versus transfer t at E_γ of 3.5 and 6 GeV*

$-t$	$p_\perp$	Θ_p	p'	Θ_ϕ	p_ϕ	$< \Theta_K <$	$< p_K <$
.03	0.00	0.0	0.17	0.0	3.33	-4.5 ; 4.5	1.24 ; 2.10
.10	0.24	-47.6	0.32	4.1	3.29	-0.4 ; 8.6	1.17 ; 2.03
.50	0.58	-49.9	0.76	10.9	3.07	6.1 ; 15.7	1.10 ; 1.90
1.0	0.78	-43.3	1.13	16.2	2.79	10.9 ; 21.5	1.03 ; 1.77
1.5	0.89	-37.4	1.46	20.8	2.50	14.9 ; 26.7	0.92 ; 1.58
2.0	0.94	-32.1	1.77	25.2	2.21	18.5 ; 31.9	0.80 ; 1.40
2.5	0.95	-27.3	2.07	29.7	1.91	22.0 ; 37.4	0.68 ; 1.22
3.0	0.90	-22.6	2.36	34.4	1.60	25.2 ; 43.6	0.56 ; 1.04
3.5	0.81	-17.9	2.64	39.5	1.28	28.0 ; 51.0	0.45 ; 0.85
4.0	0.64	-12.7	2.92	44.7	0.91	28.8 ; 60.6	0.28 ; 0.62

Table 1: *Kinematics of the reaction $\gamma + p \rightarrow p + \phi$ at E_γ = 3.5 GeV; units in GeV/c and degrees*

Center of mass angles Θ_{cm} of 90° in the (γ,p) reference frame correspond to maximum values of $p_\perp$ and transfers $t = t_{max}/2$. The kinematics of the ϕ decay in two kaons, $\phi \rightarrow K^+ + K^-$ is governed by the kaon momentum in the ϕ center of mass which is 0.128 GeV/c. Tables 1 and 2 respectively give an exhaustive list of kinematical variables for photon energies of 3.5 and 6 GeV.

$-t$	$p_\perp$	Θ_p	p'	Θ_ϕ	p_ϕ	$< \Theta_K <$	$< p_K <$
.01	0.00	0.0	0.09	0.0	5.91	-2.5 ; 2.5	2.21 ; 3.70
.10	0.28	-62.4	0.32	2.8	5.86	0.2 ; 5.3	2.19 ; 3.67
.50	0.64	-58.5	0.76	6.6	5.64	4.0 ; 9.2	2.11 ; 3.53
1.0	0.89	-51.7	1.13	9.5	5.37	6.7 ; 12.2	2.00 ; 3.37
2.0	1.18	-41.8	1.77	14.2	4.83	11.2 ; 17.3	1.80 ; 3.03
3.0	1.35	-34.8	2.36	18.3	4.28	14.8 ; 21.8	1.59 ; 2.69
4.0	1.43	-29.2	2.92	22.5	3.73	18.5 ; 26.5	1.38 ; 2.35
5.0	1.44	-24.4	3.48	26.9	3.18	22.2 ; 31.6	1.17 ; 2.00
6.0	1.38	-20.0	4.03	31.9	2.61	26.2 ; 37.6	0.96 ; 1.65
7.0	1.25	-15.8	4.57	37.9	2.03	30.4 ; 45.2	0.73 ; 1.30
8.0	1.00	-11.3	5.11	45.6	1.40	35.1 ; 56.1	0.48 ; 0.91

Table 2: *Kinematics of the reaction $\gamma + p \rightarrow p + \phi$ at $E_\gamma = 6$ GeV/c; units in GeV and degrees*

3.2 CLAS figures of merit for the proposed study

To check the feasibility of the proposed study with the CLAS detector, we made use of FASTMC [17] to evaluate resolutions and phase space acceptance. The input events are generated with OMNOU [18] according to the kinematics described above and with a flat t dependence of the differential cross-section. We assumed 100% efficiencies and disregarded trigger simulations. This seems a reasonable approach in the configuration we will use CLAS, where only scintillators are used for triggering. Because the momenta of all involved particles is well above 200 MeV/c, maximum efficiencies near 100% are awaited for each individual counter. Where K decay in flight is concerned, most of them have momenta above 0.8 GeV/c and thus less than 15% decay before hitting the scintillators. We can safely neglect this fraction for the purpose of estimates in regions of transfer t where no data exist up to now. The target characteristics used for the simulation are the following: liquid hydrogen contained in a cylindrical mylar vessel 10 cm long, 6 cm diameter and 0.5 mm wall thickness.

a)Particle identification

In it's present version, the CLAS hadron identification capabilities rely on the scintillator information, i.e. ToF identification. The scintillators being situated approximately 4 m from the target location, the ToF separation between K and π is roughly:

$$\Delta t \approx \frac{1.5ns}{p^2(GeV^2)}$$

The main background for the reaction under study in terms of single rates is the photoproduction of the ρ^0 meson: $\gamma p \rightarrow p\rho^0 \hookrightarrow \pi^+\pi^-$. It will contribute to the trigger

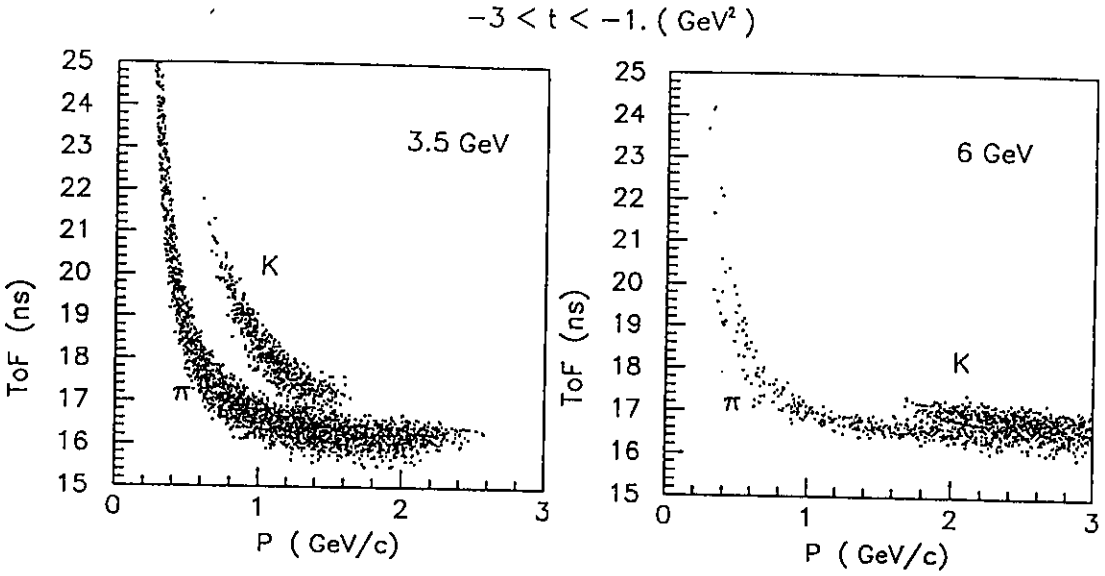

Figure 11: *Simulated ToF/momentum correlations for kaon issued from ϕ decay and background pions in a typical angular range around 25° at 3.5 GeV and 15° at 6 GeV*

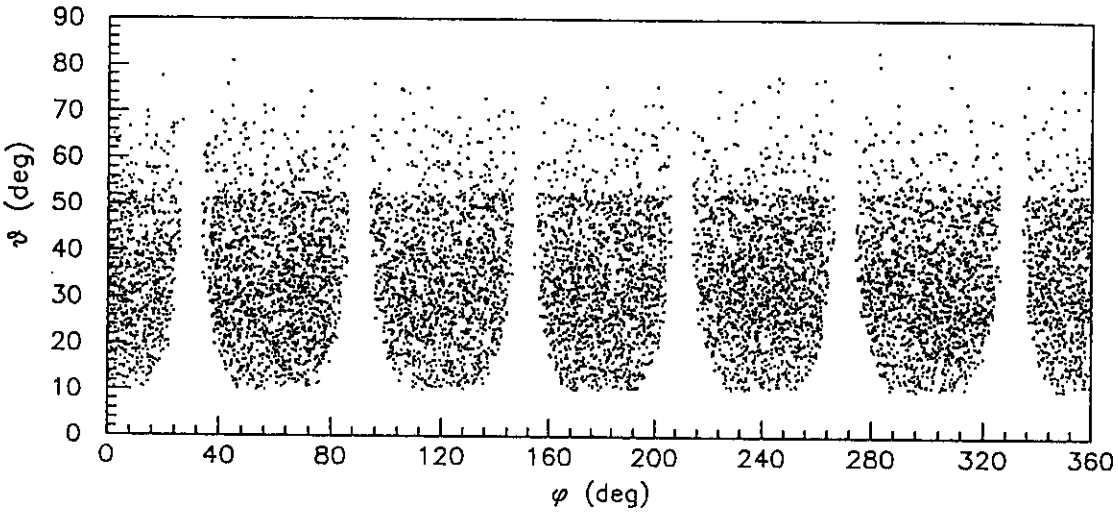

Figure 12: *Correlation Θ/Φ in the CLAS detector for the reaction $\gamma p \rightarrow p\phi$*

rates, since ToF discrimination is only possible off line.

From the kinematics of tables 1 and 2, it turns out that:

$$\Delta t \geq 500\ ps\ at\ E_\gamma = 3.5\ GeV\ for\ -t \geq 0.5 GeV^2$$
$$\Delta t \leq 500\ ps\ at\ E_\gamma = 6.0\ GeV\ for\ -t \leq 5.0 GeV^2$$

This means that π/K separation is possible at $E_\gamma = 3.5$ GeV, but is excluded with the use only of scintillators at $E_\gamma = 6$ GeV. The simulated ToF/momentum correlations for the reactions $\gamma p \rightarrow p\phi \hookrightarrow K^+K^-$ and $\gamma p \rightarrow p\pi^+\pi^-$ confirm this conclusion (figure 11).

b)Phase space

The angular range of the CLAS detector, represented by a Θ/Φ plot for generated

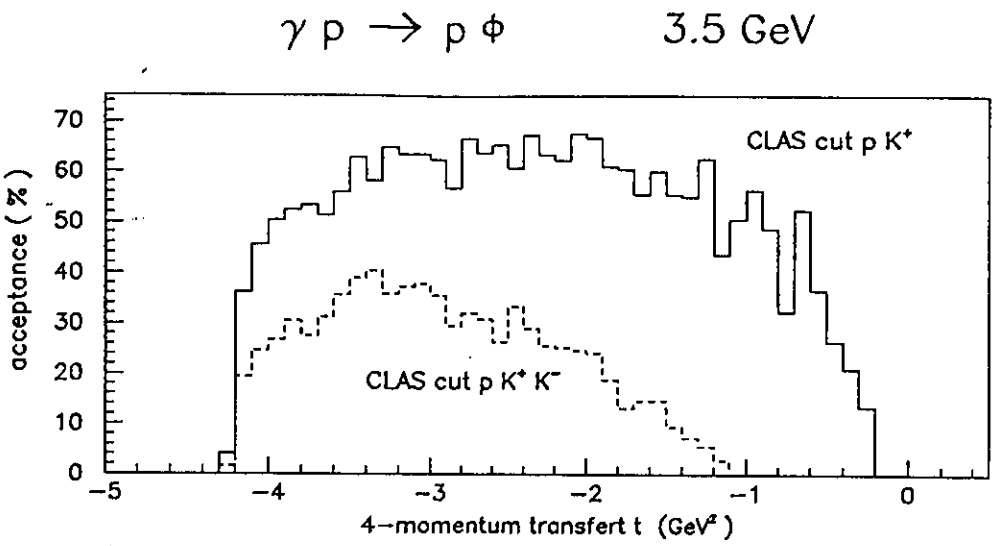

Figure 13: *CLAS phase space efficiency (in %) for the reaction $\gamma p \rightarrow p\phi \hookrightarrow K^+K^-$ at 3.5 GeV. Full line : p K^+ events detected in CLAS; dotted line : p K^+ K^- events detected in CLAS*

events on figure 12, allows for comfortable detection of the protons but reduces the phase space for kaons at small transfer $t \leq 1$ GeV^2, where they are produced at angles below 10°. The shape of the Θ/Φ plot is explained by the presence of the coils. In the configuration where the negative charged particles are bent toward the beam (our assumption), a large proportion of K^- will be lost because they escape through the forward hole. That explains the shape of the acceptance function as a function of transfer $-t$ (figure 13), showing that practically all events with $-t \leq 2$ GeV^2 are lost if we require simultaneous detection of p, K^+ and K^- in the final state. We chose therefore to rely only on the detection of the proton p and the K^+, and the following simulations of resolution and background are made with this assumption. The overall acceptance of CLAS in this case is reasonably large, about 50% at 3.5 GeV and 35% at 6 GeV.

c)Resolutions

The key parameter of the experiment with respect to background rejection is the resolution for the reconstructed mass of the ϕ and the energy balance E_{bal}. As stated above, we will focus on the reaction $\gamma p \rightarrow pK^+X$. Though knowledge of the incident photon energy and parameters of the outgoing proton are in principle enough to determine M_ϕ ($M_\phi = \sqrt{(\underline{\gamma} + \underline{p} - \underline{p'})^2}$) , using the overdetermination of the undetected particle mass $M_X = M_{K^-}$ increases the resolution:

$$\begin{cases} \vec{p}_X &= \vec{\gamma} - \vec{p}' - \vec{p}_{K^+} \\ E_X &= \sqrt{\vec{p}_X{}^2 + M_{K^-}^2} \end{cases} \Longrightarrow \begin{cases} M_\phi &= \sqrt{(E_X + E_{K^+})^2 - (\vec{p}_X + \vec{p}_{K^+})^2} \\ E_{bal} &= E_\gamma + M - E' - E_{K^+} - E_X \end{cases}$$

The energy balance E_{bal} allows kinematical separation of backgrounds involving other particles than kaons (pions e.g., see next section). The experimental resolution for these quantities is a function of the tagger resolution ($\Delta E_\gamma / E_\gamma = 0.3\%$), CLAS angular ($\Delta\Theta \approx 1$

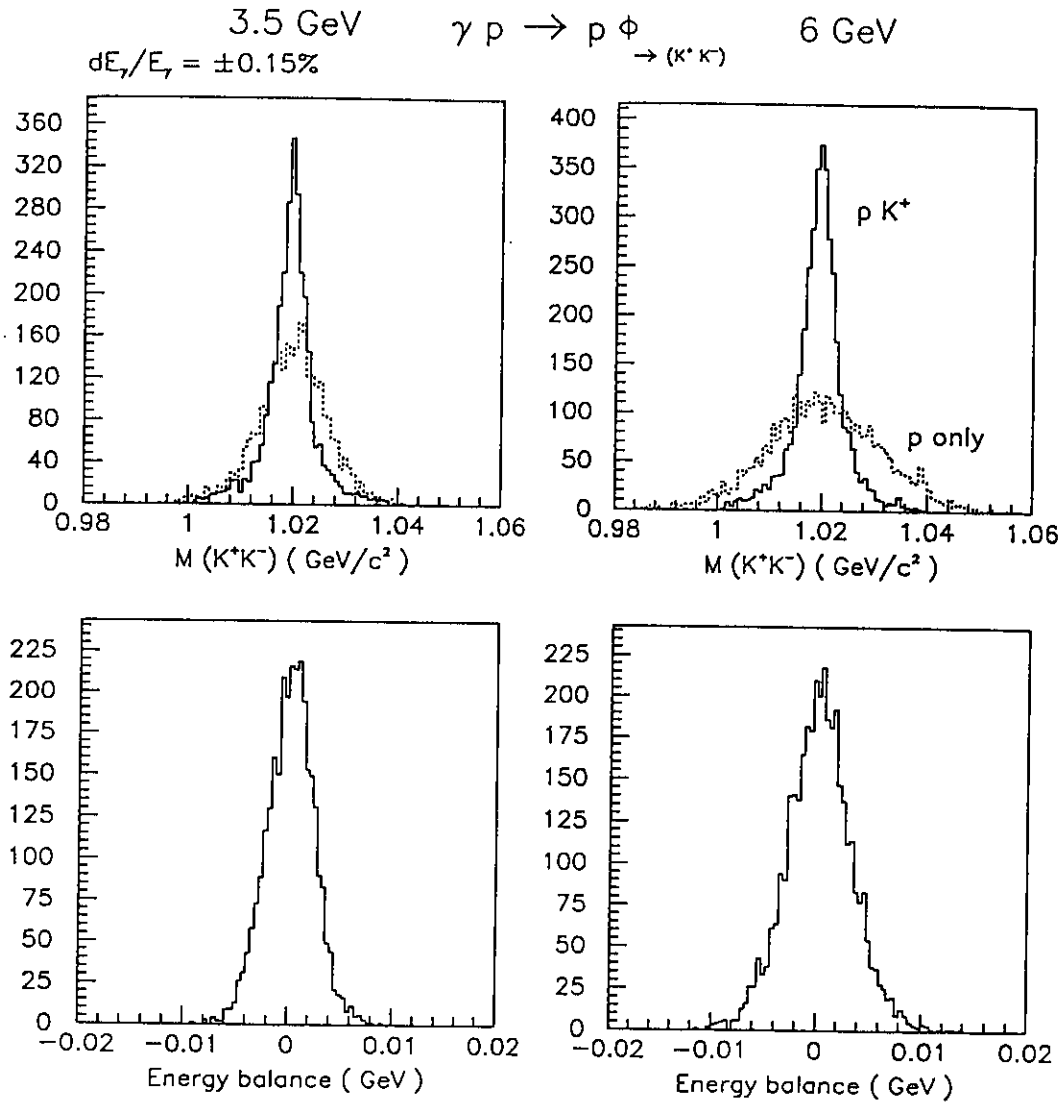

Figure 14: *Simulated M_ϕ and E_{bal} for the reaction $\gamma p \rightarrow p\phi \hookrightarrow K^+K^-$ with p K^+ detected (a,b at 3.5 GeV and c,d at 6 GeV); the dashed line corresponds to the use of only γ, p' informations (see text for explanations)*

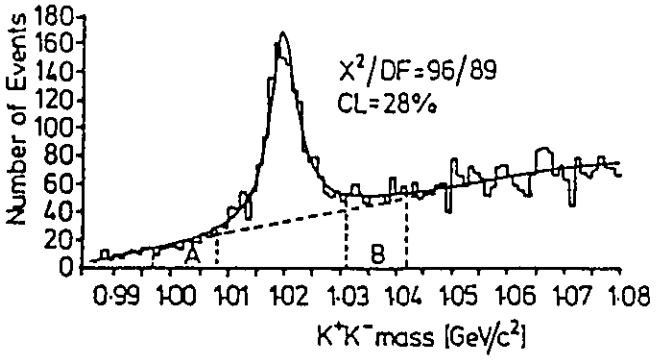

Figure 15: *Experimental $M_{K^+K^-}$ spectrum as measured at Daresbury*

msr) and momentum resolution ($0.5\% \leq \Delta p\,/p \leq 1\%$). Simulated spectra of M_ϕ and E_{bal} at 3.5 and 6 GeV photon energies are shown in figure 14. At both energies, resolutions are such that all events are inside $\Delta E_{bal} = 20$ MeV and 95% inside $\Delta M_\phi = 20$ MeV. These figures are comparable with the resolutions obtained in a previous experiment [5] and allow:
- a good estimate of the background near threshold ($M_{th} = 986$ MeV, $M_\phi = 1020$ MeV) as visible on figure 15;
- a good kinematical rejection power against backgrounds as discussed below.

3.3 Backgrounds and count rate estimates

a)Physical backgrounds

In the energy region of interest, $E_\gamma \geq 3$ GeV, the main physical backgrounds are π production ($\gamma p \rightarrow p\rho^0$,...), hyperon production ($\gamma p \rightarrow \Lambda K^+$) and non resonant K production. These can be distinguished on figure 16 which shows the simulated M_ϕ/E_{bal} correlation at $E_\gamma = 3.5$ GeV for the different backgrounds we will discuss now.

We classify them in two groups:
- the reactions where a K^+ is present in the final state: non resonant $\gamma p \rightarrow pK^+K^-$ and $\gamma p \rightarrow K^+\Lambda$
- the reactions involving π's in the final state: $\gamma p \rightarrow p\rho^0 \hookrightarrow \pi^+\pi^-$ and $\gamma p \rightarrow p\pi^+\pi^-$ (neutrals). We neglect reactions with more than three pions in the final state.

Only K backgrounds will contribute at $E_\gamma = 3.5$ GeV, pions being rejected by ToF discrimination (see section 3.2a), whereas these later have to be considered at 6 GeV where no discrimination is possible.

$\gamma p \rightarrow pK^+K^-$:

The final state particles are the same as for the studied reaction $\gamma p \rightarrow p\phi$, and the energy balance is hence the same : zero. Nevertheless, the $M_{K^+K^-}$ distribution is that of an uncorrelated 3-body phase space continuum, and thus appears as

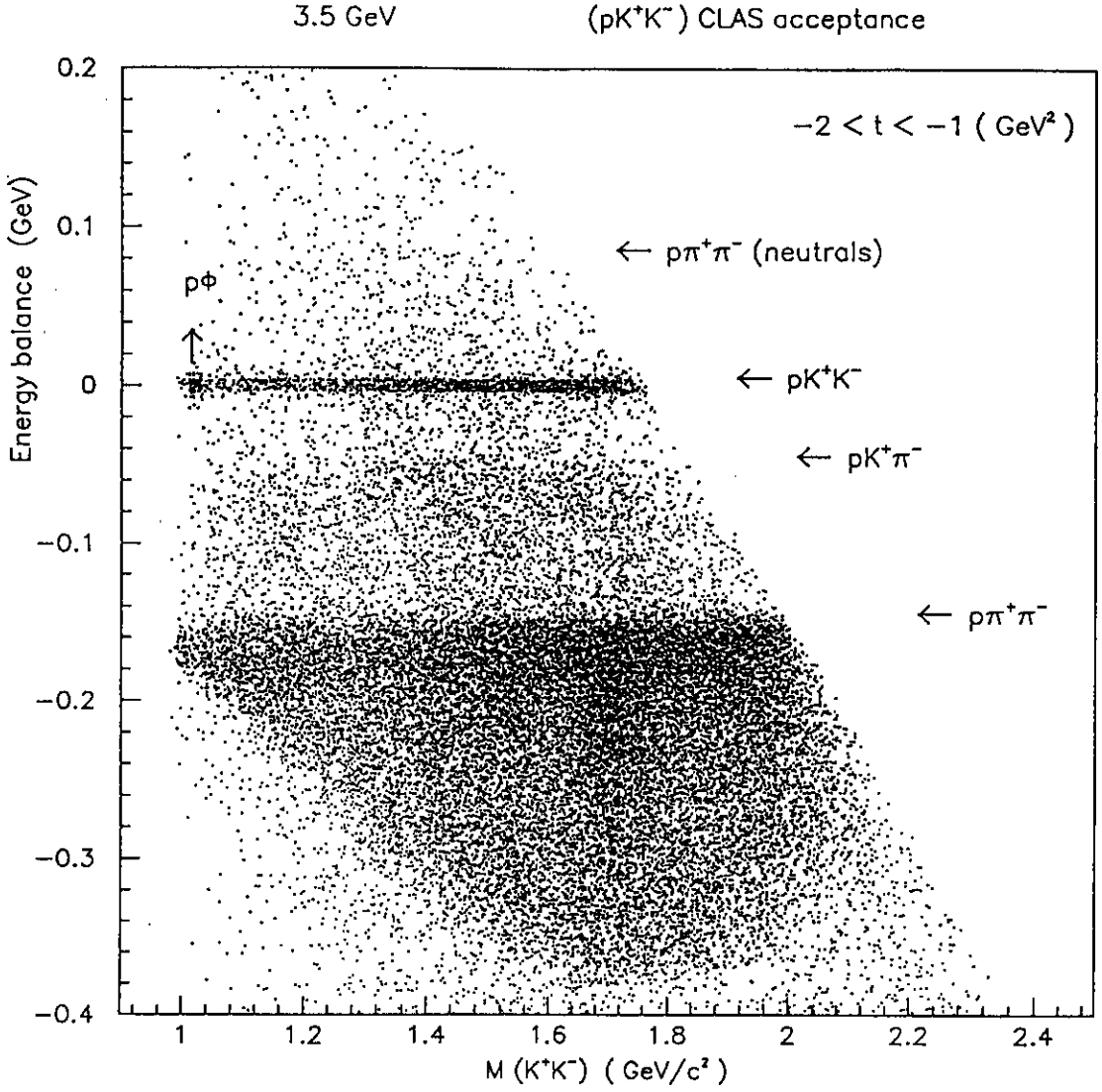

Figure 16: *Simulated M_ϕ/E_{bal} correlation at $E_\gamma = 3.5$ GeV for the $\gamma p \to p\phi$ and background reactions*

a uniform background underneath the sharp ϕ peak. The total cross section of this reaction is $\approx 1\ \mu b$ at our energies, but no experimental t-dependence is known. Experiments on two and three pion photoproduction on proton [19,24] show a definite exponential t dependence at low t. Moreover, the slope of such a dependence increases strongly with decreasing invariant mass of the multi-pion system. We will assume a 3-body phase space distribution of the pK^+K^- system with *no* and $e^{1.5t}$ dependence, although we are convinced that the *former assumption is very pessimistic and the latter remains conservative.*

$\underline{\gamma p \rightarrow K^+\Lambda \hookrightarrow p\pi^-}$:

We dispose of three criteria to discriminate this reaction from $\gamma p \rightarrow p\phi$:

- The lifetime of the Λ is such that it decays into $p\pi^-$ at about 7 cm from the interaction point, and on the average the Λ escapes at an angle of 40° with respect to the beam. If the π^- is accepted in CLAS, the vertex reconstruction allows a clean discrimination. Now for the same reasons that the K^- acceptance is small, the π^- will often be lost and this vertex criteria can only be applied on a small sample.

- Because the undetected particle is a π^-, the energy balance of this reaction is:

$$E_{bal} = \sqrt{\vec{p}^2_{\pi^-} + M^2_{K^-}} - \sqrt{\vec{p}^2_{\pi^-} + M^2_{\pi^-}} \approx M^2_{K^-}/2p_{\pi^-}$$

and hence $\geq$ 40 MeV at 3.5 GeV. Given the good energy balance resolution (figure 14),this criteria allows a clean discrimination with respect to $\gamma p \rightarrow p\phi$ as can be seen on figure 17.

-At E_γ = 6 GeV, this last criteria may be marginal due to the higher momentum of the pion. In this case, we can make use of the kinematical correlation Θ/p of the detected K^+ which is drastically different for the two reactions (figure 17).

Given the small total cross section for the reaction $\gamma p \rightarrow K^+\Lambda$ of $1.5\mu b$, the combination of the three above cited criteria will allow a clear cut discrimination against this background.

$\underline{\gamma p \rightarrow p\pi^+\pi^-}$:

At the energies of interest here, $\pi^+\pi^-$ production proceeds mainly through the reaction $\gamma p \rightarrow p\rho^0 \hookrightarrow \pi^+\pi^-$, whose total cross section is of the order of 20 μb. This is factor 20 times more than K^+K^- production, but it is very well separated from the reaction $\gamma p \rightarrow p\phi$ in terms of energy balance due to the masses of the particles involved in the final state (figure 16).

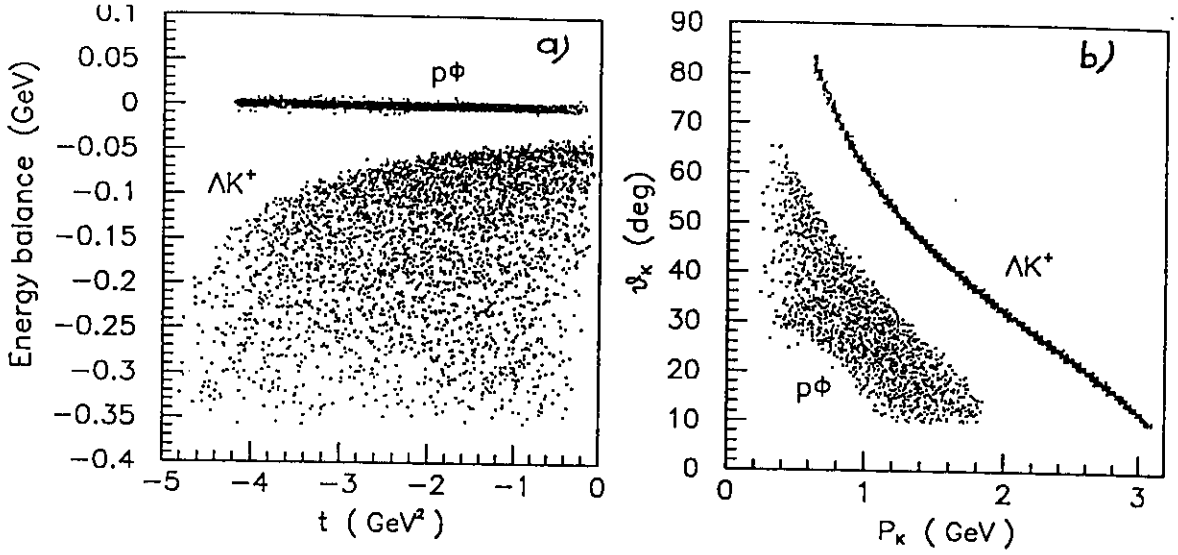

Figure 17: *Simulated a) E_{bal}/t and b) Θ/p correlations for $\gamma p \rightarrow p\phi$ and $\gamma p \rightarrow K^+\Lambda \hookrightarrow p\pi^-$ reactions at 3.5 GeV*

$\underline{\gamma p \rightarrow p\pi^+\pi^-(neutrals)}$:

In the configuration of CLAS used for the proposed experiment, neutral particles like π^0's will escape detection, and hence the energy balance of this reaction is uniformly distributed in the allowed phase space and overlaps zero. Nevertheless, even if the total cross section is 35 μb, the good energy balance resolution allows a reduction factor of about 20 when imposing a window ΔE_{bal} of 20 MeV wide. The t-dependence of this cross section is estimated from [19] to lie between: $e^{1.5t}$ and e^{3t}.

After energy balance cuts, two backgrounds survive:
- $\gamma p \rightarrow pK^+K^-$ at both 3.5 and 6 GeV
- $\gamma p \rightarrow p\pi^+\pi^-(neutrals)$ at 6 GeV.

Because they are uniformly distributed in $M_{K^+K^-}$, an additional reduction factor of about 100 occurs when imposing $\Delta M_\phi = 20$ MeV.

The reduced background cross sections $\frac{d\sigma}{dt}_{b\ red}$, obtained by multiplying the physical cross sections by the reduction factors from $\Delta E_{bal} = 20$ MeV and $\Delta M_\phi = 20$ MeV cuts, will allow us to estimate the real background rate underneath the ϕ peak.

b)$\underline{\text{Count rate estimates at 3.5 GeV}}$

We discuss count rate estimates only at 3.5 GeV; the rates at 6 GeV can be inferred in a trivial manner, the differential cross sections being more or less independent on the photon energy. The event rate per second τ in a given transfer bin Δt is related to the differential cross section $\frac{d\sigma}{dt}$ through the relation:

$$\tau = N_\gamma/s \; N_{nucleons} \; \frac{d\sigma}{dt} \; \Delta t \; acceptance(t)$$

For the reaction $\gamma p \rightarrow p\phi$, an additional factor of 0.49 has to be taken into account for the $\phi \hookrightarrow K^+K^-$ branching ratio. We assume a photon flux N_γ/s of 10^7/s in a range $3 < E_\gamma < 3.6$ GeV, an hydrogen target 10 cm long, and Δt bins .3 GeV^2 wide. Taking an average CLAS acceptance of 50% for p K$^+$ detection (figure 13), it turns out that $\tau_\phi \; (ev/hour) \approx \frac{d\sigma}{dt}_\phi \; (nb/GeV^2)$.

Concerning backgrounds, it would be misleading to directly compare ϕ and background rates, because the level of acceptable physical background depends on statistics and hence counting time T. In the limit of infinite beam time, the ϕ will at the end always come out, even if signal/noise rates are 1/100. We therefore estimate a level of detectability of the signal over the background, by requiring the signal (ϕ events) to be 3 times the r.m.s. error of the background. This leads to the condition:

$$\frac{d\sigma}{dt}_\phi \geq \frac{1}{0.49} \sqrt{\frac{d\sigma/dt_{b\ red}}{T \; N_\gamma/s \; N_{nucleons} \; \Delta t \; accept(t)}}$$

The right hand side represents the limit of detectability of the reaction $\gamma p \rightarrow p\phi$ with respect to the many body background. Such limits for the two choices of the t dependence of the K^+K^- background, previously discussed (topics 3.3.a), are shown on figure 18 assuming 400 hours of beam time, together with estimates of the cross section $\frac{d\sigma}{dt}_\phi$ issued from models discussed in section 2.2. The expected errors are statistical only ($\sqrt{N + 2F}$), but include both the ϕ peak (N) and background (F) subtraction. They are calculated in the case of an exponential dependence. It appears that 400 hours of beam time at 10^7 photons/s allow a high statistics determination of the cross section of the reaction $\gamma p \rightarrow p\phi$, at $E_\gamma = 3.5 GeV$, up to transfers $-t$ of 2 GeV^2 and possibly up to the maximum of 4.2 GeV^2 depending on the actual ϕ production cross-section and on the observed t-dependence of the non resonant K$^+$ K$^-$ production.

Expected invariant mass distributions of the two Kaon system are presented on Fig. 19, for an $e^{1.5t}$ dependence of the background at $-t = 1$ and $-t = 1.5(GeV/c)^2$, and both an exponential or a pure phase space dependence at $-t = 4(GeV/c)^2$. In the case of the conservative exponential t dependence, where the signal to noise ratios are respectively 4.5/1, 0.8/1 and 4/1, the ϕ signal appears clearly over the whole range of momentum transfer. In the most pessimistic case of a pure phase space background, this ratio is merely 1/10 and background subtraction, although still possible, becomes more tricky. However, we stress again that this last limit is quite unrealistic.

c)single and accidental rates

The remaining question is: can we afford a photon flux of 10^7/s in the range 3. $< E_\gamma <$ 3.6 GeV ?

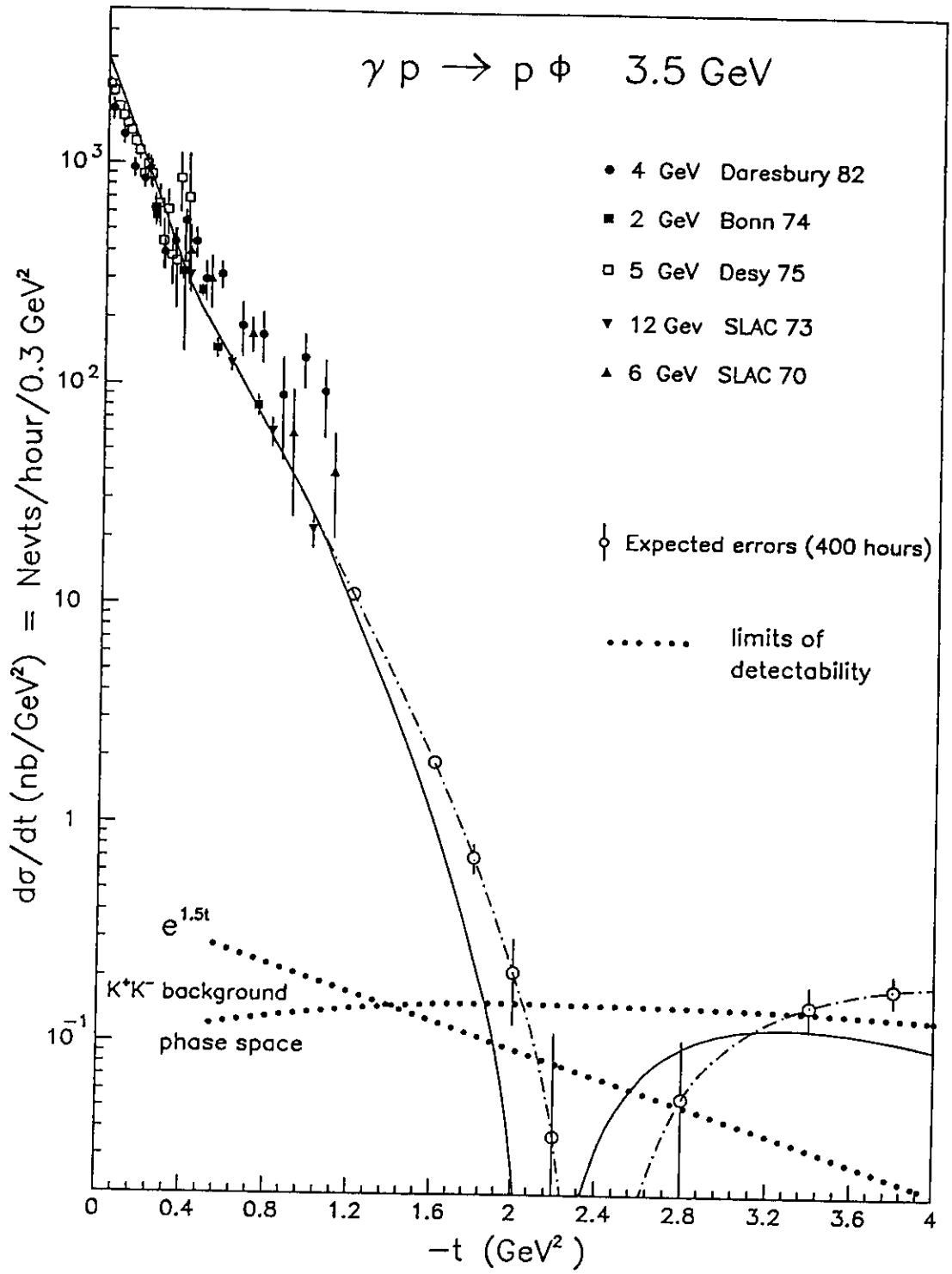

Figure 18: *Count rate estimates and limit of detectability for the reaction $\gamma p \rightarrow p\phi$ at 3.5 GeV with 400 hours beam time*

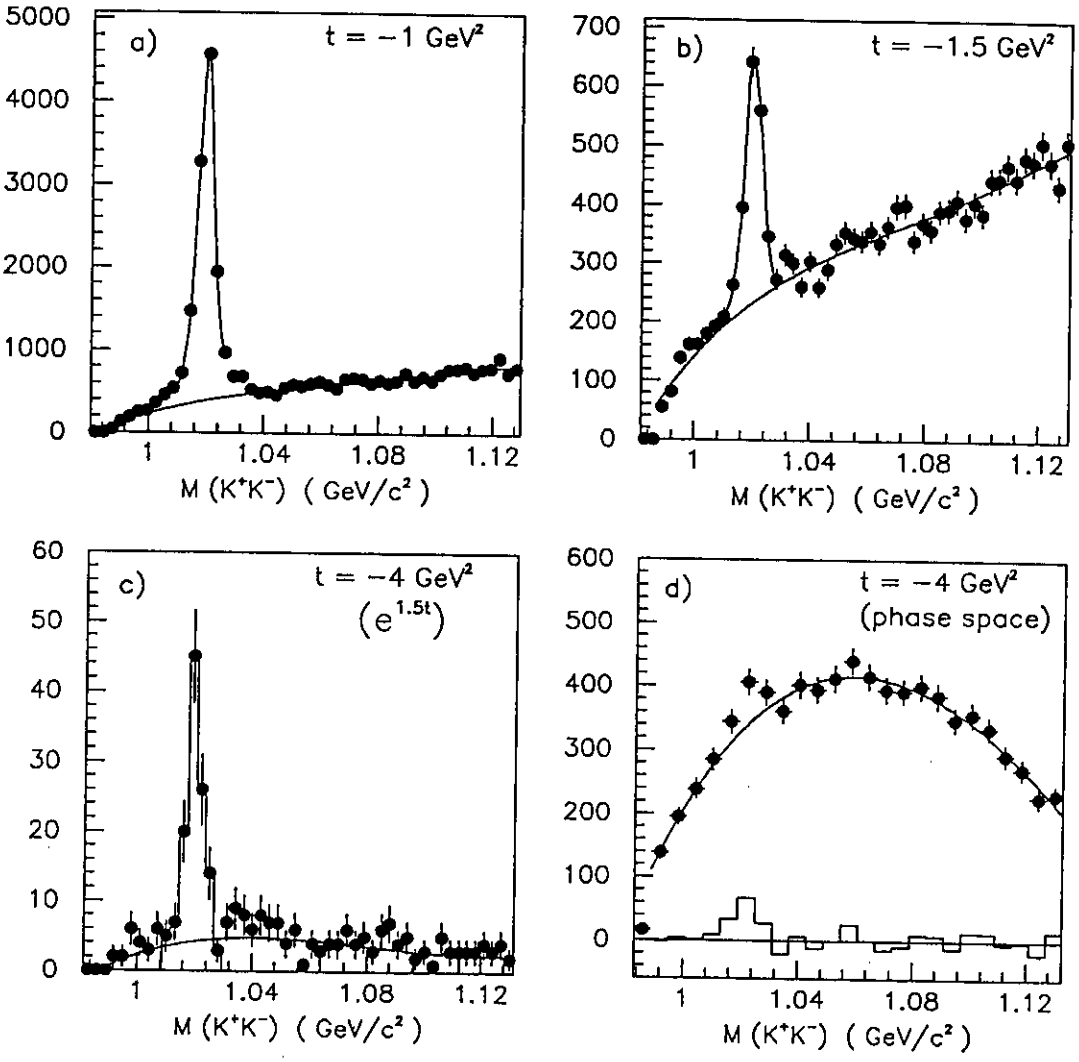

Figure 19: *Simulated two Kaon spectra at different momentum transfer t and two hypotheses on the momentum dependence of the background (see text).*

- Assuming a mean γp cross section of 300 μb in the range 0.2 - 0.5 GeV and 150 μb in the range 0.5 - 3.6 GeV, a bremssthralhung shape of $1/E_\gamma$ and a product efficiency×multiplicity of 0.5 and 1, we get a total rate of *12000 singles/s.*

- If we suppose to benefit from a trigger with two charged particles for the experiment, the main contribution to the trigger will be $\gamma p \rightarrow p\pi^+\pi^-$, whose mean cross section of 70 μb leads to a rate of *1300 triggers/s*, assuming efficiency×multiplicity of 0.3. Assuming a width of the coincidence with the tagger of 20 ns, that leads to an overall rate of *300 coincidences/s* between the tagger and the trigger.

3.4 ϕ Production in Few Body Systems

In the $\gamma D \rightarrow \phi pn$ reaction, the simultaneous detection in CLAS of the pK^+ system does no longer overdetermines the kinematics, while the detection of the pK^+K^- system does. This is the only possibility to determine the recoil neutron momentum, although the CLAS efficiency is reduced (see section 3.2).

In the $\gamma {}^3He \rightarrow \phi ppn$ reaction, the simultaneous detection of the ppK^+ system does not overdetermine the kinematics, but fixes the nucleon recoil momentum in the two body subprocess. The momentum of the spectator neutron (or equivalently the momentum of the active pp pair in the ${}^3He$ ground state) is not known, but the average over its Fermi motion reduces the problem to the study of ϕ meson production on a pp pair almost at rest in ${}^3He$: the γ"pp" $\rightarrow pp\phi$ reaction.

In view of the above considerations, the study of the $\gamma {}^3He \rightarrow \phi ppn$ reaction seems more appealing. This choice is also justified on theoretical grounds.

From the experimental point of view, the problems are much the same as for the reaction $\gamma p \rightarrow p\phi$. The reconstructed mass M_ϕ will be slightly broadened by the Fermi motion of the target pp pair, without changing the clean signature of the ϕ peak at transfer below $-t \simeq 2(GeV/c)^2$. Only a small reduction of the phase space will occur, due to the detection of two protons with approximately the same energy.

The relevant quantity to study is the momentum distribution of the recoil nucleon. According to Fig. 18, integrating the free nucleon cross-section between $1 \leq -t \leq 2(GeV/c)^2$ leads to $\simeq$ 25 events/hours or 10000 events in 400 hours. Within the same momentum transfer bin, the integral, over the recoil proton momentum, of the quasi free contribution to the cross section of the $\gamma {}^3He \rightarrow npp\phi$ reaction is :

$$\int_{-1}^{-2} dt \int d\vec{P}_R \left. \frac{d\sigma}{d\vec{P}_R dt} \right|_{q.f} \simeq \text{ 10000 events per 400 hours} \qquad (3.10)$$

Assuming a 1% probability for the hidden color component and a enhancement factor (Eq.2.9) around 3 to 4, the integral, over the recoil proton momentum, of its contribution is :

$$\int_{-1}^{-2} dt \int d\vec{P}_R \left. \frac{d\sigma}{d\vec{P}_R dt} \right|_{cc} \simeq \text{ 300 to 400 events per 400 hours} \qquad (3.11)$$

If we take 10 bins of $\Delta P_R \simeq 0.2 GeV/c$, it is possible to map out the tail of the recoil momentum distribution, in the range $0 \leq P_R \leq 2 GeV/c$, with 30 to 40 events/bins within 400 hours.

At higher values of the momentum transfer ($t > 2(GeV/c)^2$), it will be only possible to measure contributions integrated on t as well as on P_R, with an accuracy depending on the actual sizes of the two gluon exchange contribution and the two kaon emission background.

3.5 The reaction $\gamma p \rightarrow K^+\Lambda$

As it is apparent in Fig. 17, the $\gamma p \rightarrow pK^+\Lambda$ channel is clearly identified and clearly separated from the $\gamma p \rightarrow p\phi$ channel. The corresponding events will be recorded at the same time as the ϕ events and the corresponding cross-section will be obtained. Although we have not made any attempt to simulate this particular channel in CLAS, it is clear that the unique combination of a high energy tagged photon beam and an overdetermined kinematics in a large acceptance detector will allow us to map out the corresponding cross-section in a large part of the phase space. More particularly, the high momentum transfer events will be especially interesting regarding our study of hard mechanisms : they are expected to be mostly sensitive to the onset of quark rearrangement mechanisms involving the strange quarks of the sea.

4 Experimental feasibility and counting rate for the reactions $\gamma + p \rightarrow p + \rho$ and $\gamma + p \rightarrow p + \omega$

The experimental feasibility of the ρ photoproduction measured in CLAS has been carefully investigated performing a simulation of the experiment. To this purpose two main programs have been used :

- A special code has been developped [20] to generate events corresponding to the interaction of monochromatic photons with the proton in the energy range from 0.3 up to 6 GeV. All possible channels with pion multiplicity up to 6 have been included. The total cross section of each channel has been taken from experimental data [19,21]. For $E_\gamma \leq 2.5 GeV$, the differential cross sections of the ρ and Δ^{++} production channels have been modeled [22] in the framework of the Söding model [23]. For higher energies, the more realistic measured angular distributions have been used. For $p\pi^+\pi^-$ phase space total cross section, the experimental value obtained in ref. [19] has been used, while a t dependence of the form $\exp(at)$ was utilized to weight the events as suggested by this experiment.

- FASTMC [17] program has been used to evaluate efficiencies and resolutions as measured in CLAS. Simulations have been performed at $E_\gamma = 2$, 3.5 and $4.7 GeV$. Kinematics, particle identification, beam and target characteristics, magnetic field intensity

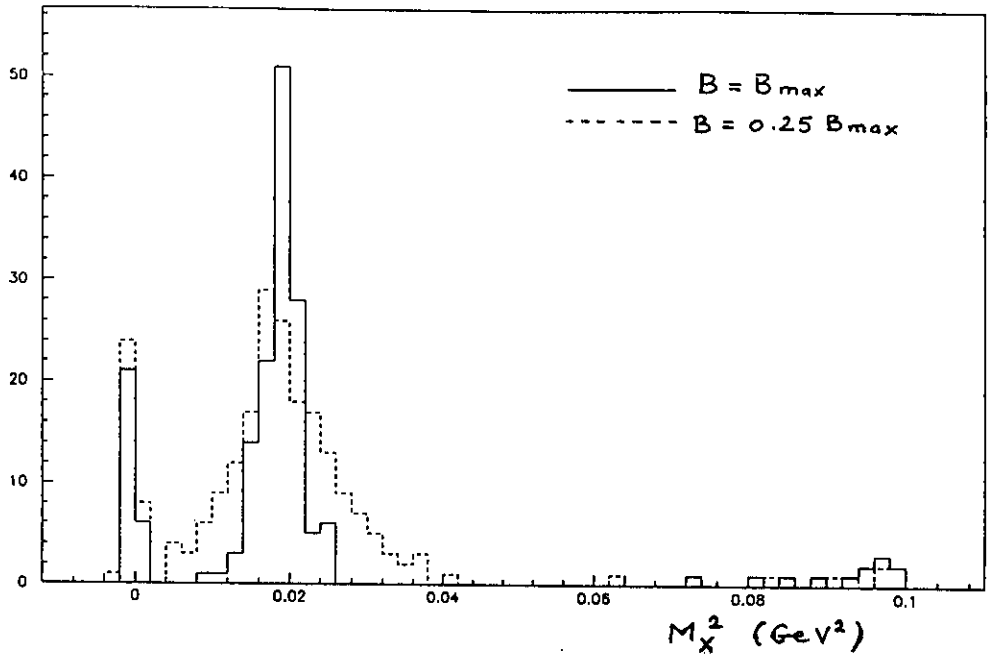

Figure 20: *Missing mass spectrum M_X^2 in the reaction $\gamma p \rightarrow p\pi^+\pi^- X$ at $E_\gamma = 2GeV$ for two magnetic field settings.*

and polarity are the same as described in sections 3.1 and 3.2 for ϕ production.

4.1 Resolution

In our configuration we assume that negative charged particles are bent toward the beam: a large portion of the π^- produced in the ρ decay are therefore lost in the forward hole of CLAS and the efficiency for the simultaneous detection of a $p\pi^+\pi^-$ in the final state is strongly reduced. In ϕ photoproduction, where no large background is present and where the width of the resonance is small, the efficiency has been enhanced, relying only on the detection of the proton and the K^+. This condition is not, however, applicable to the ρ production where a simple detection of a $p\pi^+$ pair appears to be inadequate to disentangle the signal from the large background of the multipion final state channels. We have therefore required the simultaneous detection of a $p\pi^+\pi^-$: the losses in the efficiency are easily compensated by the high value of the expected counting rate as well as by a clean signature of the event.

In Fig. 20, the reconstructed missing mass spectrum M_X^2 in the reaction $\gamma p \rightarrow p\pi^+\pi^- X$ is reported at $E_\gamma = 3.5GeV$ for two values of the magnetic field: $B = B_{max}$ and $B = 0.25B_{max}$.

Three regions can be singled out :

1. $M_X^2 \leq 0.005GeV^2$: the strong peak at $M_X^2 \simeq 0$ is associated to $\pi^-\Delta^{++}$, $\pi^+\Delta^0$, $p\rho^0$ and $p\pi^+\pi^-$ phase space events. This peak is well separated from the second region.

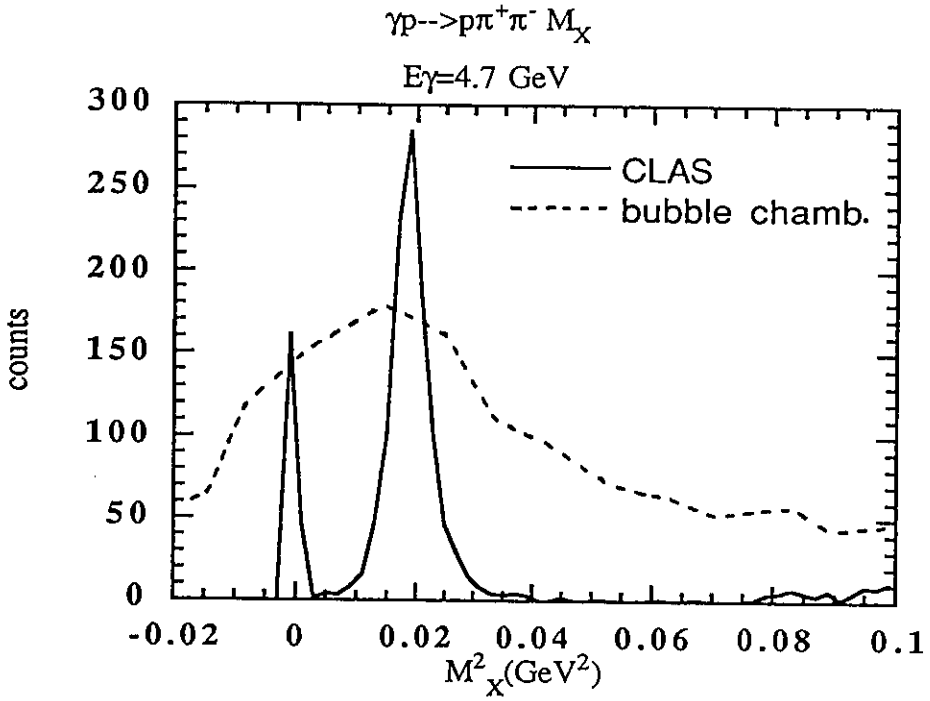

Figure 21: *Same as Fig. 20 at $E_\gamma = 4.7GeV$. The FASTMC simulation (continuous curve) is compared with bubble chamber data (dashed).*

2. $0.01 \leq M_X^2 \leq 0.03GeV^2$: it corresponds to $M_X = \pi^0$, i.e. to $\gamma p \rightarrow \omega p$ and to $\gamma p \rightarrow p\pi^+\pi^-\pi^0$ phase space events.

3. $M_X^2 \geq 0.07GeV^2$: it corresponds to multipion final state reactions, like $\gamma p \rightarrow p\pi^+\pi^-\pi^+\pi^-$, and is clearly separated from the other two.

The effect of the intensity of the magnetic field in the missing mass reconstruction is clearly evident from the comparison of the continuous curve ($B = B_{max}$) to the dashed one ($B = 0.25B_{max}$). The small decrease of the area of the peak close to $M_X^2 \simeq 0$ for $B = B_{max}$ corresponds to a 20% damping in the detection efficiency of the $\gamma p \rightarrow p\pi^+\pi^-$ channel. However this effect is largely compensated by the increase of the overall resolution, indicating that the condition $B = B_{max}$ is adequate also for the ρ photoproduction measurement.

The same simulation with $B = B_{max}$ has been performed at $E_\gamma = 4.7GeV$ in order to investigate the mass reconstruction at higher energies as well as to compare with previous existing bubble-chamber experiments [24]. In Fig. 21, our FASTMC simulation is plotted together with these data : the improvement on the quality of the measurement is very impressive.

In CLAS the peaks corresponding to $M_X \simeq 0$, $M_X \simeq \pi^0$, $M_X \simeq \pi^+\pi^-$ ... are clearly separated, indicating that this large acceptance detector is the ideal one to study vector meson photoproduction.

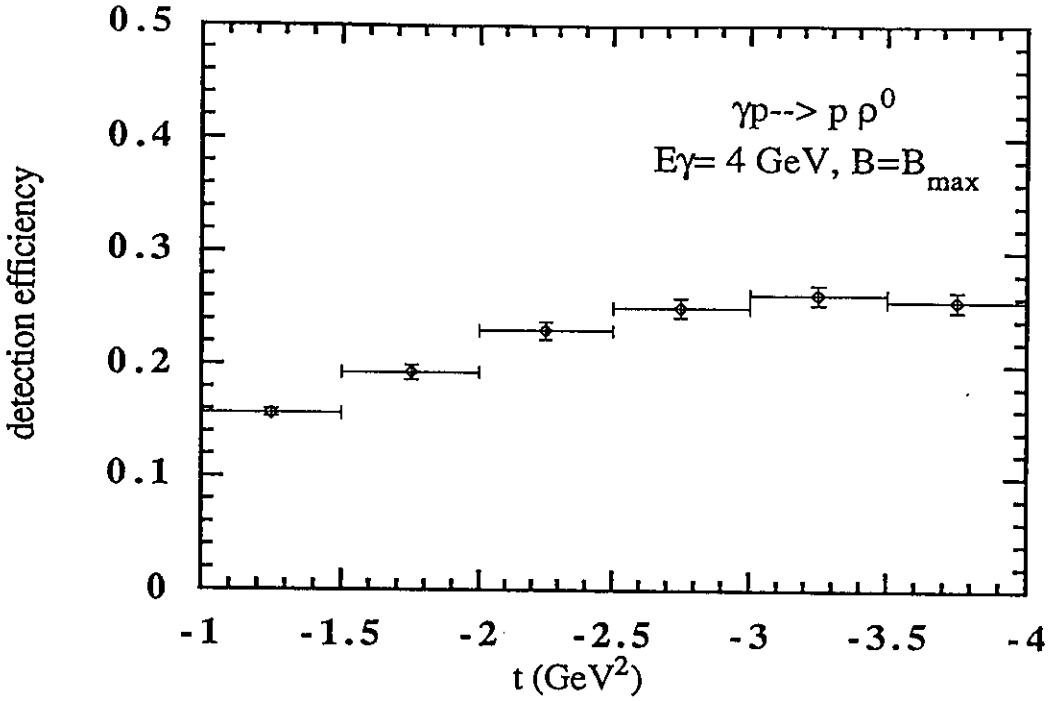

Figure 22: *Simulated detection efficiency for $\gamma p \rightarrow p\rho^0$ when $p\pi^+\pi^-$ are simultaneously detected.*

4.2 Efficiency

The previous simulations on the missing mass reconstruction have shown that a clear identification of the $p\pi^+\pi^-$ channel can be obtained when considering all the events with $M_X \simeq 0$. In Fig. 22, the detection efficiency for these events is reported as a function of the momentum transfer t : the photon energy is $3.5GeV$ and the magnetic field is maximum.

At $-t < 2(GeV/c)^2$ a decrease of the acceptance from its average value of 25% is observed : at these momentum transfer the ρ meson is emitted at small angles where most of the π^- from its decay are bent toward the beam and lost in the forward hole. This reduction is not, however, important since we are primarily interested in the production of the ρ meson at high momentum transfer, and not in the diffractive part.

4.3 Mass reconstruction

As we have discussed above, $p\pi^+\pi^-$ events can be unambiguously reconstructed in CLAS in all our photon energy range. The contributions to this two charged pion final state are the following: $\pi^-\Delta^{++}$, $\pi^+\Delta^0$, $p\rho^0$ and $p\pi^+\pi^-$ phase space. It is therefore important to quantify how the reconstructed mass of the ρ emerges out of the other two pion channels.

Theoretical assumptions [23], as well as experimental data, indicate that the two pion phase space can be described by a Drell process where a t dependence in the form $\exp(at)$ ($a > 0$) is expected. In our simulations we have therefore extracted the events according to

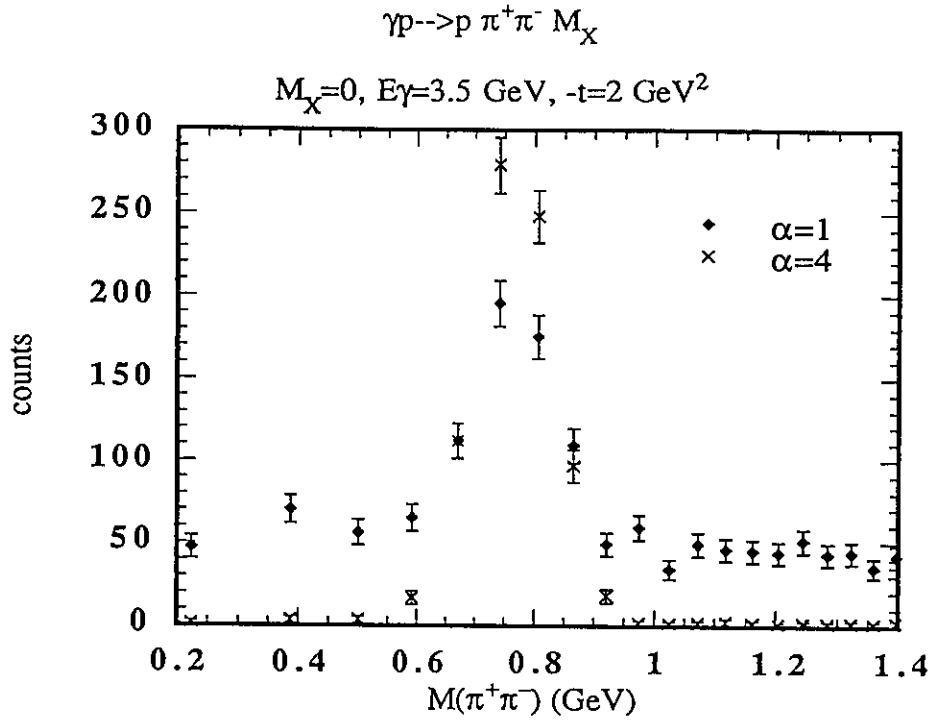

Figure 23: *Effective-mass distribution $M(\pi^+,\pi^-)$ for the $\gamma p \to p\pi^+\pi^-$ channel. The phase space contribution has been weighed with* $\exp(at)$ *with $a = 1(GeV/c)^{-2}$ and $a = 4(GeV/c)^{-2}$.*

the experimental cross-section of ref. [19] with two different values of the coefficient a for the phase space: $a = 4(GeV/c)^{-2}$ as the average of the data of Ref. [19] and $a = 1(GeV/c)^{-2}$ as a conservative value.

The result of a simulation at $E_\gamma = 3.5GeV$ and $t = -2(GeV/c)^2$ is reported in Fig. 23, where the invariant mass of the $\pi^+\pi^-$ pair clearly shows the peak of the ρ both for $a = 1(GeV/c)^{-2}$ and $a = 4(GeV/c)^{-2}$. This identification is expected to last also for higher values of $-t$, if the phase space contribution continues to decrease exponentially.

Finally, it is worth it to note that ω mesons can also be detected in parallel to ϕ and ρ events. The spectra of the reconstructed missing mass for the reaction $\gamma p \to p\pi^+\pi^- X$, reported in Figs. 20 and 21, show a sharp peak for $0.01 \leq M_X^2 \leq 0.03GeV^2$ where only $\gamma p \to \omega p$ and $\gamma p \to p\pi^+\pi^-\pi^0$ events are present. Our simulation indicates, however, that only a few per cent of the events relative to the ω peak ($\Gamma \simeq 10MeV$) are present in the reconstructed $\pi^+\pi^-\pi^0$ invariant mass spectrum. It turns out that the π^- from the ω decay are almost completely lost.

The simultaneous detection of a $p\pi^+\pi^0$ system seems, instead, a more promising way to measure the cross-section of the reaction $\gamma p \to \omega p$, with an efficiency of the order 5 to 10%. Fig. 24 shows the simulated spectrum of the $\pi^+\pi^-\pi^0$ squared invariant mass when a proton, a positive pion and at least one the two photons from the neutral pion are simultaneously detected. The contributions to the large continuous background include

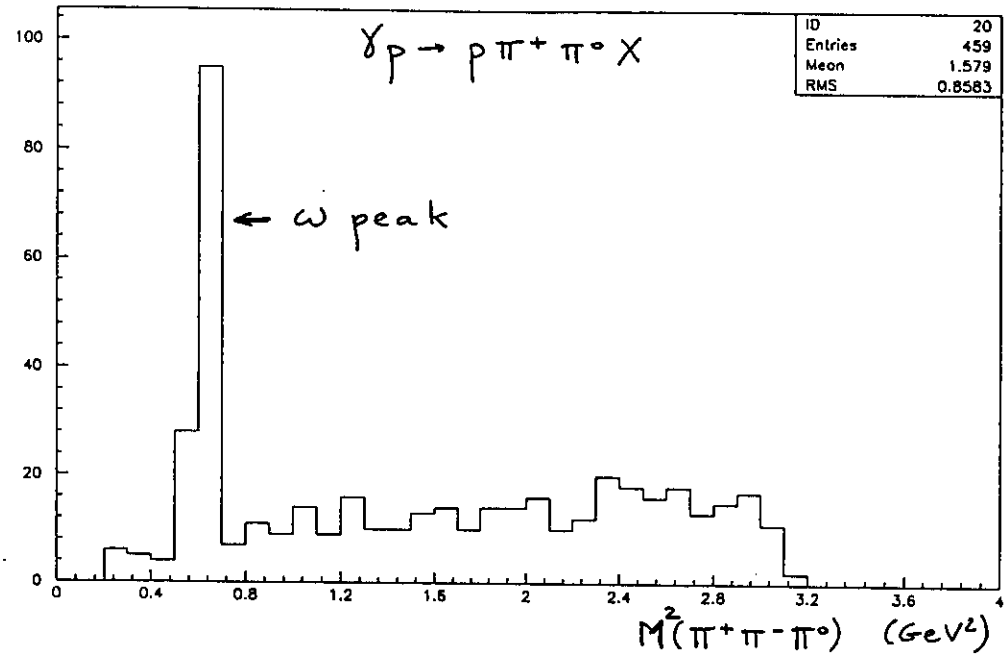

Figure 24: *Simulated squared effective-mass distribution* $M^2(\pi^+\pi^-\pi^0)$ *at* $E_\gamma = 3.5GeV$.

$p\pi^+\pi^-\pi^0$ phase space and other multipion final state channels. In this case the phase space events are always strongly present; nevertheless the small width of the ω resonance and the good momentum resolution of the CLAS detector seem to allow a good determination of the ω production channel.

4.4 Counting rate

Counting rate estimates can be easily obtained from the relation reported in section 3.3. The value of the cross section for the $\gamma p \rightarrow \rho p$ channel is about 10 to 100 times larger than the cross-section of the $\gamma p \rightarrow \phi p$ channel. Assuming the same target thickness and the same photon flux, it turns out that the ρ production cross section can be determined with few per cent statistical accuracy, within the requested beam time assignment.

5 Beam request

We require a total amount of 800 hours of tagged photon beam in Hall B. This beam request does not include any time devoted to the tune-up of either CLAS or the tagger and any time for contingencies.

The lower limit of the tagger will be set at approximately $3\,GeV$, and $10^7\,\gamma/s$ will be used in the range $3 \leq \Delta E_\gamma \leq 3.6\,GeV$ at the nominal CEBAF energy ($4\,GeV$). A liquid

cryogenic target, designed in Saclay, will be installed in CLAS.

A first period of 400 hours will be devoted to the study of the production of vector mesons on the nucleon at high momentum transfer. The main emphasis will be put on ϕ meson production, but the production of ρ meson as well as of $\pi^+\pi^-$ or K^+K^- pairs in the continuum will be studied at the same time.

A second period of 400 hours will be devoted to the study of the $^3He(\gamma, 2p\phi)n$ reaction. Again two Kaons and two Pion events will be recorded at the same time.

Depending on the success of these studies, an additional period will be requested in due time to complete them by the study of the $D(\gamma, p\phi)n$ reaction.

6 Conclusion

For the first time the combined use of a continuous electron beam and a large acceptance detector offers the opportunity to undertake a comprehensive study of vector meson photoproduction at high P_T : an almost virgin field. Special emphasis will be put on the ϕ meson sector which will allow us to investigate the t dependence of two gluon exchange mechanisms : their static and global properties are already advocated in the analysis of nucleon nucleon scattering at very high energies or the analysis of the nucleon structure functions at small x.

The simulation of this channel in the CLAS detector shows that the study of the $p(\gamma, \phi)p$ reaction is straightforward for $1 \leq -t \leq 2(GeV/c)^2$: this considerably extends the presently known domain and allows us to see the onset of two gluon exchange mechanisms. Assuming a reasonable t dependence of the $2K$ non resonant background, this study is possible for higher values of t (up to $t \simeq 4(GeV/c)^2$ at $E_\gamma = 3.6\,GeV$: it is here that two gluon exchange mechanisms or other hard mechanisms are expected to clearly manifest themselves. However, the determination of the t dependence of this non resonant background presents also its own interest regarding its coupling to possible exotic states (a_0 and f_0 resonances, $K\overline{K}$ molecules, ...).

The study of the ρ meson production sector needs more kinematical constraints, due to its large width. However, its production cross section is much larger than for the ϕ meson : this compensates the corresponding losses in the efficiency. The 2π events will be recorded together with the $2K$ events, and the comparison of the energy variation of ρ and ϕ meson production cross sections with the energy as well as the momentum transfer will be a powerful way to disentangle two gluon exchange mechanisms and quark interchange mechanisms.

The two gluon exchange mechanisms provide us with a unique way to unravel possible hidden color components in the wave function of the few body systems, or more generally short range correlations between quarks. Although a detailed knowledge of these quantities is not available today— the goal of this experiment is to improve it— a rough estimate shows that the corresponding counting rate is expected to be comparable to counting rate

[19] ABBHHM collaboration, *Phys.Rev.* **175** (1968) 1669;
Phys. Rev. **188** (1969) 2060.

[20] P.Corvisiero, L.Mazzaschi , *private communication.*

[21] Cambridge bubble chamb. group, *Phys. Rev.* **155** (1967) 1477.

[22] M. Ripani, *private communication.*

[23] P. Söding, *Phys. Lett.* **8** (1966) 702.

[24] J.Ballam *et al.*, *Phys. Rev.* **D5** (1972) 545.

in the study of free nucleon, provided a suitable binning of the events. In many respects, the reaction $^3He(\gamma,\phi 2p)n$ seems to be particularly appealing.

References

[1] J.M. Laget, "Strangeness Production in Intermediate Energy Scattering" (Lectures given at the 5^{th} Summer School on Nuclear Physics, Seoul, June 29—July 4, 1992), *Journal of the Korean Physical Society* **26** (1993) S244.

[2] J.M. Laget, "Probing the Short-Range Behavior of Nuclei with High P_T Photo- and Electro-Nuclear Reactions", *Lectures Notes in Physics* **365** (1990) 77.

[3] P.V. Landshoff, *Nucl. Phys.* **B** (Proc. Suppl.) **18C** (1990) 211.

[4] H.J. Behrends *et al.*, *Nucl. Phys.* **144** (1978) 22;
D.C. Fries *et al.*, *Nucl. Phys.* **143** (1978) 408.

[5] D.P. Barber *et al.*, *Z. Phys.* **C12** (1982) 1.

[6] J.R. Cudell, *Nucl. Phys.* **B336** (1990) 1.

[7] A. Donnachie and P.V. Landshoff, *Phys. Lett.* **B185** (1987) 403;
Nucl. Phys. **B311** (1988/89) 509.

[8] P.V. Landshoff and 0. Nachtman *Z. Phys.* **C35** (1987) 405.

[9] D.G. Cassel *et al.*, *Phys. Rev.* **D24** (1981) 2787.

[10] J.J. Aubert *et al.*, *Phys. Lett.* **B161** (1985) 203.

[11] F. Cannata, J.P. Dedonder and L. Lesniak, *Z. Phys.* **A334** (1989) 457.

[12] J. Weinstein and N. Isgur, *Phys. Rev.* **D41** (1990) 2236;
Phys. Rev. **D43** (1991) 95.

[13] R. Jaffe, *Phys. Rev.* **D15** (1977) 267.

[14] J.M. Laget and R. Mendez-Galain, *in preparation.*

[15] R.L. Anderson *et al.*, *Phys. Rev.* **D14** (1976) 679.

[16] Y. Yamauchi and M. Wakamatsu, *Nucl. Phys.* (1986) **A457** 621.
A.M. Kusainov, V.G. Neudatchin and I.T. Obukhovsky, *Phys. Rev.* **C44** (1991) 2343.

[17] E.S. Smith, "Fast Monte Carlo Program for the CLAS detector", CLAS-NOTE-90-003, 1990.

[18] OMNOU, P-Y. Bertin, private communication.